The 2006 Eruption of Augustine Volcano, Alaska
Power, J.A., Coombs, M.L., and Freymueller, J.T., editors
U.S. Geological Survey Professional Paper 1769

Chapter 22

High-Resolution Satellite and Airborne Thermal Infrared Imaging of the 2006 Eruption of Augustine Volcano

By Rick L. Wessels[1], Michelle L. Coombs[1], David J. Schneider[1], Jonathan Dehn[2], and Michael S. Ramsey[3]

Abstract

Thermal infrared (TIR) images provided a timely pre- and syn-eruption record of summit changes, lava flow emplacement, and pyroclastic-flow-deposit distribution during the Alaska Volcano Observatory's (AVO) response to the 2006 eruption of Augustine Volcano. A series of images from both handheld and helicopter mounted forward looking infrared radiometers (FLIR) captured detailed views during a series of 13 overflights from December 2005 through August 2006. In conjunction with these images, data from the Advanced Spaceborne Thermal Emission and Reflection Radiometer (ASTER) provided frequent multispectral synoptic views of the eruption's emissions and deposits. The ASTER Urgent Request Protocol system also facilitated more frequent scheduling and faster data availability during the eruption. Airborne and satellite imaging provided 20 different days of TIR coverage over the 5-month eruptive period, with 4 of those days covered by both FLIR and ASTER. The high-resolution TIR images documented gradual pre-eruption heating of the summit, emplacement of pyroclastic-flow deposits, rapid temperature increase as the lava dome and flows formed, and slow cooling of the volcanic deposits that followed. The high-resolution data uniquely documented segmentation of the lava flows into hot areas of increased flow deformation and cooler, more stable crust on the active flows. In contrast, the satellite TIR data provided synoptic views of the areal distribution of volcanic products at Augustine including the extent and composition of the plumes.

Introduction

Thermal infrared (TIR) imaging of active volcanoes has increasingly become an important tool for monitoring and documenting dynamic volcanic processes. The Alaska Volcano Observatory (AVO) routinely monitors all volcanoes in the North Pacific using low-spatial-resolution (kilometer scale), high-temporal-resolution (multiple images per day) TIR data from the Advanced Very High Resolution Radiometer (AVHRR), Moderate Resolution Image Spectrometer (MODIS), and Geostationary Operational Environmental Satellites (GOES) (Harris and others, 1997; Dehn and others, 2002; Wright and others, 2002; see Bailey and others, this volume). Whereas these data work well for detecting gross thermal changes and large ash plumes that precede and accompany eruptions, higher-spatial-resolution data are commonly required to detect lower temperatures and the subtle changes that are common during ongoing volcanic phenomena (fig. 1). Satellite sensors, such as the Advanced Spaceborne Thermal Emission and Reflection Radiometer (ASTER) and the Thematic Mapper (TM)/Enhanced Thematic Mapper (ETM+) on Landsats 5 and 7, respectively, provide high-spatial-resolution (tens of meters), low-temporal-resolution (days to weeks) TIR data (Flynn and others, 2001; Ramsey and Dehn, 2004; Vaughan and Hook, 2006; Carter and others, 2008). Airborne or ground-based TIR imaging radiometers provide a very high spatial resolution (centimeters to meters) with a variable temporal resolution depending on the study (Harris and others, 2005; Ball and Pinkerton, 2006). High-resolution TIR images can document precursory changes in existing thermal features, such as fumaroles or hot springs, as well as track structural changes indicated by the formation of new fumaroles, hot fractures, and (or) the melting of snow and ice (Schneider and others, 2000; Andronico and others, 2005). Both satellite and airborne TIR images can also be used to effectively observe eruption plumes (see Bailey and others, this volume), to document lava dome and flow dynamics and effusion rates (Ramsey and Dehn, 2004; Harris and others, 2005), and to document pyroclastic flow emplacement (Carter and others, 2007).

[1] Alaska Volcano Observatory, U.S. Geological Survey, 4200 University Drive, Anchorage, AK 99508.

[2] Alaska Volcano Observatory, Geophysical Institute, University of Alaska Fairbanks, P.O. Box 755905, Fairbanks, AK 99775.

[3] Department of Geology and Planetary Science, University of Pittsburg, Pittsburg, PA 15260.

After more than 10 months of increasing seismicity, deformation, gas emission, and heat flow, Augustine Volcano, Alaska (fig. 1), explosively erupted on January 11, 2006. The volcano produced a total of 13 explosions during the last 3 weeks of January 2006. A new summit lava dome and two short, blocky lava flows were emplaced from February to March. A series of 13 forward looking infrared radiometer (FLIR) over-flights and 7 daytime and 15 nighttime Advanced Spaceborne Thermal Emission and Reflection Radiometer (ASTER) scenes were acquired in response to this activity. The FLIR and ASTER data provided several significant observations as part of a much larger suite of real-time or near-real-time data from other satellite (AVHRR, MODIS), airborne (visual, gas), and ground-based (seismometers, global positioning system [GPS], radiometers) sensors used at AVO (see Bailey and others, this volume; Cervelli and others, this volume, Coombs and others, this volume; McGee and others, this volume; Power and Lalla, this volume).

In this chapter, we summarize airborne FLIR observations acquired between December 2005 and August 2006 and the longer record of spaceborne ASTER observations acquired between December 2000 and May 2006. The high-resolution FLIR data document the gradual pre-eruption heating of the summit, the formation of pyroclastic-flow deposits, the rapid increase in temperature as the lava dome and flows formed, and the slow cooling of volcanic deposits after the eruption. In addition to these observations of the eruption, the ASTER data provide a baseline from which to examine temperature trends over several years leading up to and during the most recent volcanic unrest.

Instrumentation and Methodology

FLIR Surveys and Data Processing

The primary airborne imaging system used in this study consists of a FLIR Systems ThermaCAM PM595 infrared camera and a Sony EVI-370 NTSC video camera housed in a helicopter-mounted four-axis gyrostabilized gimbal (see Schneider and others, 2008, for system details). A handheld version of the PM595 camera was used for repeat ground-based time-lapse imaging. The infrared camera utilizes a 320×240 microbolometer detector array, which is sensitive from 7.5–13 µm, converting TIR emitted radiance into brightness temperature. The gimbal-mounted system has an integrated 12º lens with a horizontal field of view of 210 m and a pixel resolution of 65 cm at a distance of 1 km; the handheld system has an integrated 24º lens with a horizontal field of view of 420 m and a pixel resolution of 1.3 m at a distance of 1 km. The observation distance of each survey ranged from 0.5 to 5 km, averaging about 1.2 km. The measured FLIR brightness temperature is captured by using one of three ranges, −40 to 120ºC, 80 to 500ºC, and 350 to 1,500ºC. In the low

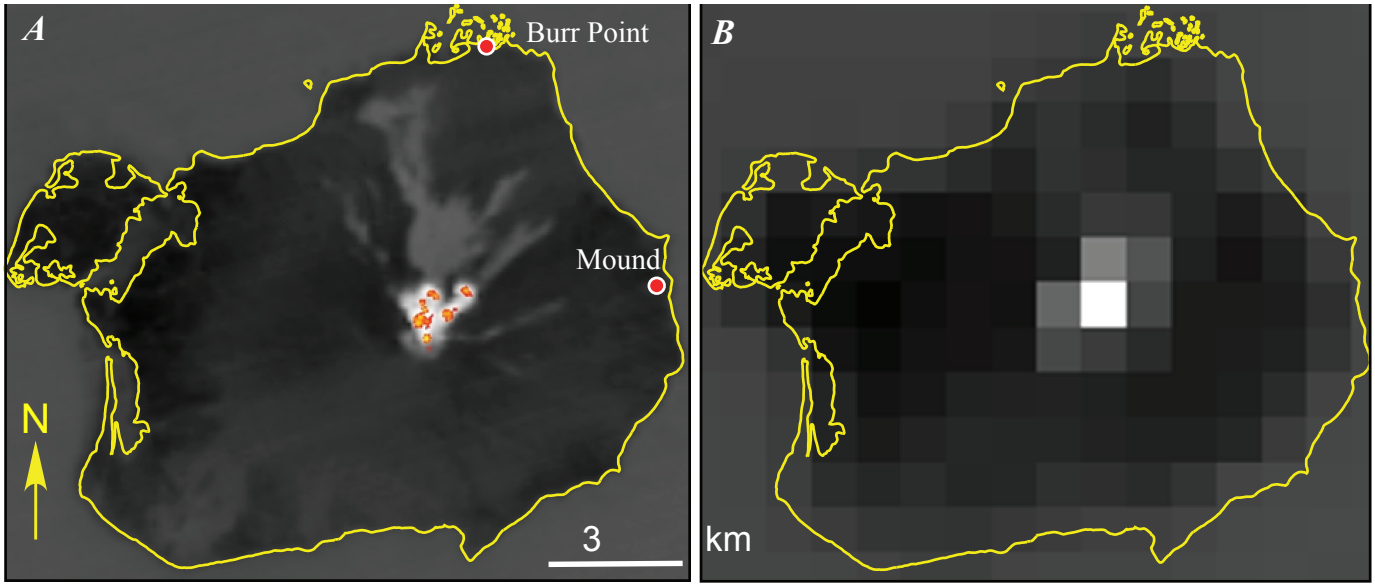

Figure 1. Nighttime 8.3-µm thermal infrared (TIR) images of Augustine Volcano acquired at 2245 AKST March 13, 2006, from the Terra spacecraft, oriented with north up. *A*, Advanced Spaceborne Thermal Emission and Reflection Radiometer (ASTER). *B*, Moderate Resolution Imaging Spectroradiometer (MODIS). Both MODIS and the Advanced Very High Resolution Radiometer (AVHRR) have ~1-km spatial resolution, which provides high-temporal-resolution views of North Pacific volcanic activity; however, these datasets lack sufficient spatial detail to capture persistent, low-level thermal features, smaller-scale activity, and eruptive deposits, are captured by ASTER TIR (90 m) and shortwave infrared (SWIR) (30 m) images.

range, the camera can record a maximum temperature of about 270ºC, but these measurements can be much less accurate because they fall outside the calibrated range. Because the temperatures measured at Augustine range from cool (ambient) to very hot (fumaroles/lava), no single PM595 gain setting covers the full range of possible temperatures, and so surveys were typically collected in at least the lower two dynamic ranges. For the FLIR temperatures reported here (see figs. 2, 5–12, 14–16), the color bar represents a linear scaling of most of the data, not the full temperature range; the lowest temperatures are clipped to black, and the highest are clipped to white.

Both the internal FLIR camera firmware (ThermaCAM PM595 Operator's Manual, 1999) and the FLIR desktop ThermaCAM Researcher software (ThermaCAM Researcher User's Manual, 2004) can convert the detected radiance to temperature-at-surface by making a first-order correction for atmospheric absorption and emission. The distance to target, ambient air temperature, relative humidity, and broadband emissivity of the surface must be inputted. Air temperature and humidity were measured onsite during each overflight. The distance to target was calculated from the difference between the time-synced GPS helicopter position and the estimated position of the feature being imaged. FLIR data were acquired during helicopter flights by several different flight crews as weather and volcanic activity permitted. For each flight, the track was recorded by using a hand-held GPS unit. The GPS tracking data provided the location and altitude at the time of the data collection, which allowed the distance to target to be calculated. The first flights conducted a general survey of the volcanic edifice and then focused on thermal changes at the summit. As the eruption progressed, later flights surveyed the fresh pyroclastic flow deposits and lava flows. Oblique aerial photographs and videos were acquired simultaneously for comparison with the TIR images. Although dates and times for geophysical data are typically recorded in UTC, we use Alaska standard time (AKST) (UTC+9) hours throughout this chapter (unless noted) to match other chapters in this volume. Alaska daylight time, which was in effect after March 21, is 1 hour later than AKST.

Satellite Data Acquisition and Processing

Visible and infrared satellite imaging of volcanoes needs to be frequent to record rapid changes in activity and to compensate for the obscuration by any heavy/recurring cloud cover. The primary high-resolution satellite-based TIR data used for this work were recorded by ASTER, which was launched in December 1999 onboard the Terra satellite. ASTER measures the top of atmosphere radiance in 14 spectral channels (Yamaguchi and others, 1998) that are collected by three subsystems, each at a different spatial resolution: the visible and near infrared (VNIR) sensor with three channels (0.56–0.81 μm) at 15-m spatial resolution, the shortwave infrared (SWIR) sensor with six channels (1.65–2.4 μm) at 30-m spatial resolution, and the TIR sensor with five channels (8.2–11.3 μm) at 90-m spatial resolution. ASTER TIR data saturate if the detected radiance exceeds a value that corresponds to a pixel-integrated brightness temperature of ~97°C. In these datasets, the at-sensor radiance from the higher-resolution SWIR channels was used to extract pixel-integrated brightness temperatures >100°C. We note that since January 2009, data from the SWIR sensor are no longer usable, owing to a failed cryocooler; however, the five TIR channels were used to extract most of the ASTER-derived temperatures presented in this chapter. Hot areas on active lava flows are typically smaller than the area covered by 90-m TIR pixels. As a result, the radiance measured is an area-weighted sum of the multiple-subpixel radiating components (Wright and Flynn, 2003). Depending on the magnitude difference of the measured temperatures, this averaging can produce a large underestimation or overestimation of the actual derived temperatures and errors in the surface emissivity (Rose and Ramsey, 2009). Therefore, the temperatures derived from mixed radiance data are commonly denoted as pixel-integrated temperatures.

The ASTER TIR data analyzed in this chapter are derived from the calibrated, at-sensor radiance. These data must first be corrected for atmospheric absorption/emission by using a standard atmospheric model with specific corrections for the image location and the time of year of acquisition (Thome and others, 1998). To then extract the pixel-integrated brightness temperatures from the atmospherically-corrected radiance, the downwelling sky radiance reflected off the surface must be removed, and the surface temperature separated from the emissivity in each pixel. These steps are applied in the temperature-emissivity separation (TES) standard data processing (Gillespie and others, 1998). The Level-2 Surface Kinetic Temperature product data distributed by the National Aeronautics and Space Administration (NASA) Land Processes Distributed Active Archive Center (LP DAAC) are presented here.

Observations and Results

Frequent FLIR missions before and during the 2006 eruption of Augustine Volcano provided detailed views of summit thermal features and fresh volcanic deposits (table 1). In this section we describe the key observations from FLIR TIR images acquired over 13 different overflights, as well as from ASTER data acquired before and during the eruption. A time series of FLIR images viewed from the same point north of the volcano show some of the changes to the volcanic edifice from January 9 to March 15, 2006 (fig. 2). For example, the January 9 images (figs. 2*A*, 2*B*) show the pre-eruption melting of the summit snow cover and warm air above caused by rising steam, and the February 24, images (figs. 2*C*, 2*D*) show the initial stages of the new summit lava dome and the north lava flow. These images also detect pyroclastic-flow deposits (unit Cpf, fig. 2) from late January, which are still warm. The March 10 (figs. 2*E*, 2*F*) and March 15 (figs. 2*G*, 2*H*) images detect a much larger lava dome and clear progression of the two lava flows.

Table 1. Summary of FLIR data for Augustine Volcano acquired 2005–2006.

Date	Time (AKST)[1]	FLIR: Tmax (°C)[2]	FLIR: Tbg (°C)[3]	FLIR: Tavg (°C)[4]	Observations (after Coombs and others, this volume)	Observation quality
December 22, 2005	1509	210	−3	5	Snow-covered summit and flanks; no flowage deposits; some increased heat flow and fumarole activity at summit	Summit partially obscured by steam
January 4, 2006	AM+PM	380	−5	0	Snow-covered flanks; no flowage deposits; maximum summit temperature at fumarole; overall heating of summit region	Summit partially obscured by steam
January 12, 2006	1204	121	−5	3	Ash from Events 1 and 2 on north flank; new vent visible through 1986 dome, just south of 1986 spine	Summit partially obscured by steam and ash plume
January 24, 2006	1229	140	−15	10	Fresh snow on summit and flanks, light ash on SE flank; dark, hot, steaming, levied flows on E, NE, and N flanks; ExD1 visible on east part of summit, Tmax 140°C	Summit mostly obscured by lenticular cloud
February 8, 2006	1149	120	−1	11	Dark Cpf and RPpf flows on north flank in high contrast to fresh white snow, range from 10−25°C with some bigger, hotter blocks.	Summit mostly obscured by lenticular cloud
February 20, 2006	AM+PM	277	0	40	Good views of Cpf, RPpf; EfLf dome and north flow visible especially in FLIR images	Summit mostly obscured by low cloud deck
February 24, 2006	1519	277	−13	38	Excellent views of summit, including north lava flow	Summit partially obscured by steam
March 10, 2006	AM+PM	700	−10	66	Clear views of both NE and N lava flows; active block-and-ash flows down East Chute and from front of NE lava flow	Summit partially obscured by light steam and ash
March 15, 2006	0953	335	−5	47	Both north and NE lava flows thickened and lengthened compared to March 10; rockfall activity and ash emission diminished	Summit partially obscured by steam
March 26, 2006	AM+PM	221	−2	16	No major changes from last observation; lava-flow fronts still hot, no significant temperature changes	Summit partially obscured by steam and clouds
April 6, 2006	AM+PM	652	−1	8	Lava-flow fronts cooler, flow tops similar as compared to previous surveys; lava-flow dimensions unchanged; Summit vent atop dome very hot (650°C)	Fresh snow has covered many deposits
May 13, 2006	0956	432	4	14	North-south linear trend of fumaroles and mineralization at summit; images of all flowage deposits; summit vent cooled to 432°C	Very clear summit views; rock sampling
August 7, 2006	1030	377	12	15	North-south linear trend of fumaroles and mineralization at summit; summit vent cooled to 377°C	Very clear summit views; rock sampling

[1]Overflight and field work typically span one-plus hours and are generally midday;

[2](Tmax) maximum pixel-integrated temperature (a value of 277 indicates FLIR gain setting was saturated);

[3](Tbg) FLIR-derived background temperature;

[4](Tavg) average surface temperature of of warm ground or active lava areas.

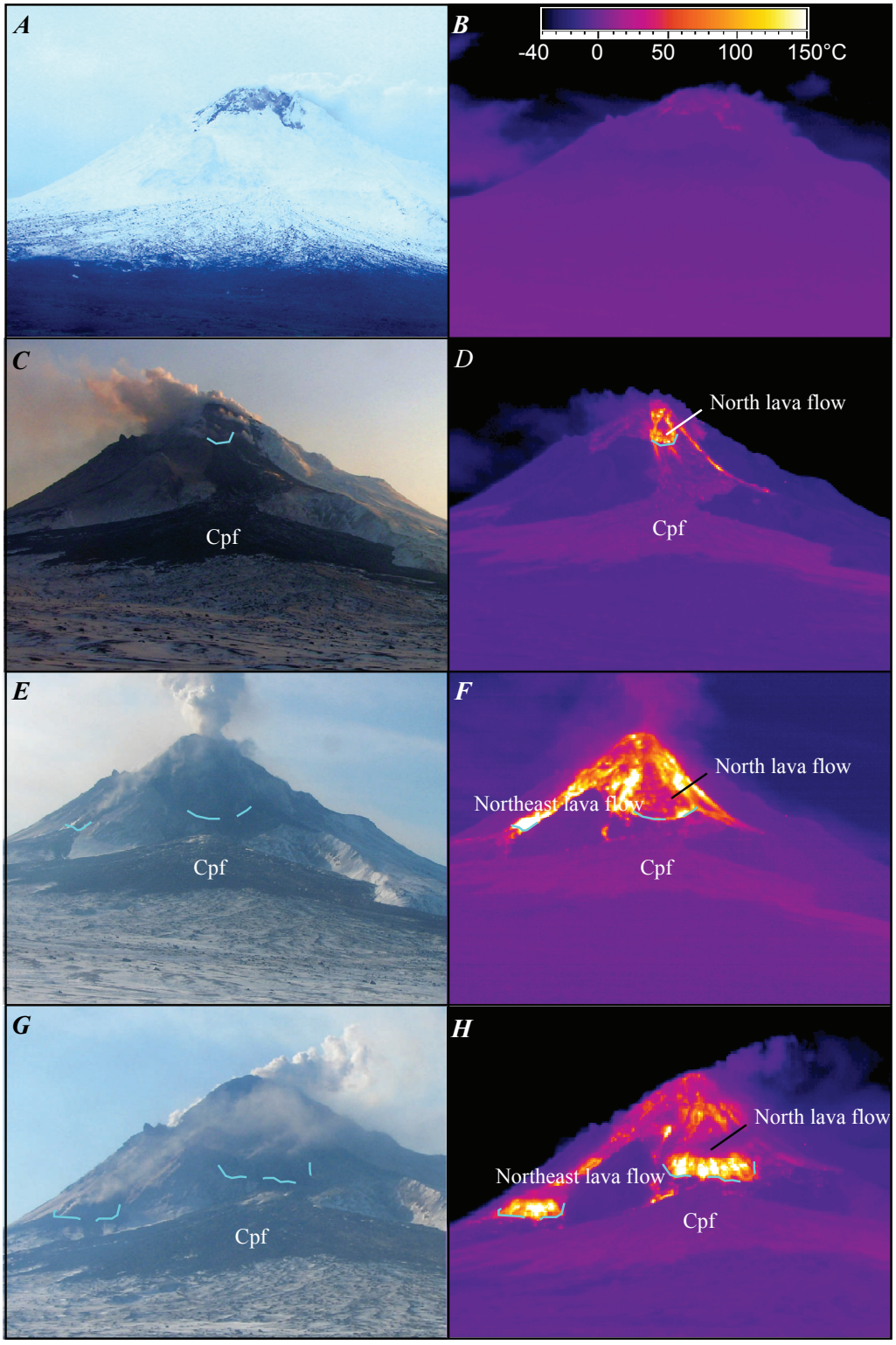

Figure 2. Photographs and Forward Looking Infrared Radiometer (FLIR) thermal infrared (TIR) images documenting growing thermal areas and new lava flows on Augustine Volcano. *A,B*, January 4, 2006. *C,D*, February 24, 2006. *E,F*, March 10, 2006. *G,H*, March 15, 2006. Images were acquired from Burr Point, which is on the coast 4.5 km north of summit (see fig. 1*A*). View southward. Cyan dashed lines denote approximate terminus of lava. Cpf pyroclastic-flow deposit.

Table 2. Summary of Advanced Spaceborne Thermal Emission and Reflection Radiometer (ASTER) data for Augustine Volcano acquired 2005–2006.

Date	Time (AKST)	Day/ night[1]	SWIR-Tmax (°C)[2]	TIR-Tmax (°C)[2]	TIR: Tbg (°C)[3]	TIR: Tavg (°C)[4]	Observations (after Coombs and others, this volume)	Scene quality
December 20, 2005	12:37:00	day	NA	−8.8	−13	−9.5	Summit area warmed above background, snow-free areas	Thin clouds, but can see island.
January 12, 2006	12:42:44	day	NA	NA	NA	NA	Plume extending south from summit	Summit obscured by volcanic plume and thin clouds
January 24, 2006	22:44:25	night	95	3	−18	−4	TIR and SWIR thermal features at summit. Weaker TIR features on flanks	Mostly clear
January 31, 2006	22:50:44	night	408	98	−18	25.4	RPpf and smaller NW flank Cpfs visible; surface to east of RPpf obscured by plume	Summit and NE flank obscured by gas and ash plume
February 22, 2006	12:37:03	day		98	−13	25.8	Good views of new dome and pf deposits	
March 13, 2006	22:45:18	night	463.9	98	−7	63	Extents of two lava flows and hottest areas within them match up well with low-light camera images from the same night	Mostly clear
April 5, 2006	22:51:30	night	239.5	13	−11	−3.5	Summit and deposits warm, small SWIR anomaly still at summit	Mostly clear
April 27, 2006	12:37:30	day	NA	NA	NA	NA	Dark lava and pf flows on summit and north flank in high contrast to fresh white snow	Partly cloudy with high cirrus over east part of island
May 17, 2006	22:45:16	night	194.5	20	−3	5.7	Summit and pf deposits still warm, but no active lava	Clear view
May 29, 2006	12:37:25	day	NA	36.7	17	19	Summit and pf deposits still warm	Clear image
October 15, 2006	22:51:16	night	174.7	8.4	−5	1.2	Average flow temps cooler, though summit fumarole still hot	Clear image

[1]Day images have VNIR, SWIR, and TIR data, night images have on SWIR and TIR;

[2](Tmax) maximum pixel-integrated temperature from SWIR and TIR;

[3](Tbg) TIR-derived background temperature;

[4](Tavg) average surface temperature of 2006 lava areas.

In addition to routine data acquisition by ASTER, the ASTER Urgent Request Protocol (URP) system (Ramsey and others, 2004) greatly improved the number of scheduled data acquisitions. A total of 25 ASTER scenes were acquired between October 30, 2005, and May 30, 2006 most during the height of activity from late January to mid-March. The volcano was clear to partly cloudy in 13 scenes, 10 of which were adequate for extracting TIR temperatures (fig. 3; table 2). During the 5 years preceding the 2006 eruption, ASTER averaged about one scene per month over the volcano.

Precursory Phase

Beginning in April 2005, an increase in the number of earthquakes below Augustine Volcano was detected by the on-island seismic network operated by AVO (see Jacobs and McNutt, this volume; Power and Lalla, this volume) and shallow inflation beneath the summit was first detected in June 2006 (Cervelli and others, 2006). By November 2005, summit GPS stations detected that this inflation had rapidly increased (Cervelli and others, 2006). In December 2005 and early

January 2006, increased seismicity and SO_2 output, as well as phreatic explosions, all suggested that volcanic unrest was intensifying (Power and others, 2006).

Of the 18 ASTER images acquired during 2005, a daytime image from December 20 (fig. 4) was the only partly clear TIR view of Augustine before the 2006 eruption. Thin cirrus-cloud cover prevented accurate TIR temperature retrievals from either the SWIR or TIR data. However, these data show a broad area of slightly elevated TIR radiance (fig. 4*C*), which corresponds to snow-free areas and fumaroles at the summit (figs. 3*A*, 4*A*). The two bright linear features visible in the SWIR image (fig. 4*B*) may represent the warmer, snow-free areas or fumarole plumes visible in the VNIR image (fig. 4*A*).

The first FLIR reconnaissance mission, which was conducted on December 22, 2005 (fig. 5), was the first of two flights during the precursory phase of the eruption. Several linear zones of warm bare rock were detected and active steaming was seen from several new fumaroles at the summit (figs. 5*A*, 5*B*). One warm (10ºC above background), snow-free area formed over a preexisting checkerboard pattern on the east side of the summit (figs. 5*C*, 5*D*). The maximum FLIR-derived temperature of a fumarole along the northeast edge of the 1986 dome was 80ºC, with a background temperature of −5ºC (figs. 5*E*, 5*F*). Fumaroles along the 1964 scarp ranged from 60 to 80ºC, and a vigorously jetting fumarole (informally referred to as Teapot) on the south flank below the summit at about 1,150-m elevation had a maximum temperature exceeding 210ºC (figs. 5*G*, 5*H*).

Photographs and FLIR images from January 4, 2006, show that the snow-free and steaming areas had expanded westward and covered more of the summit (figs. 6*A*, 6*B*). FLIR-derived pixel-integrated brightness temperatures of the snow-free areas ranged from 20 to 50ºC. The temperature of the fumarole along the northeast edge of the 1986 dome had increased to at least 380ºC, although thermal emission was likely attenuated somewhat by persistent steam (figs. 6*C*, 6*D*). The fumarole emissions had a yellow-green tint in the visible wavelengths, most likely due to reaction of SO_2 and H_2S to form native sulfur. Teapot was no longer jetting, and maximum temperatures had decreased significantly to 45ºC (figs. 6*E*, 6*F*).

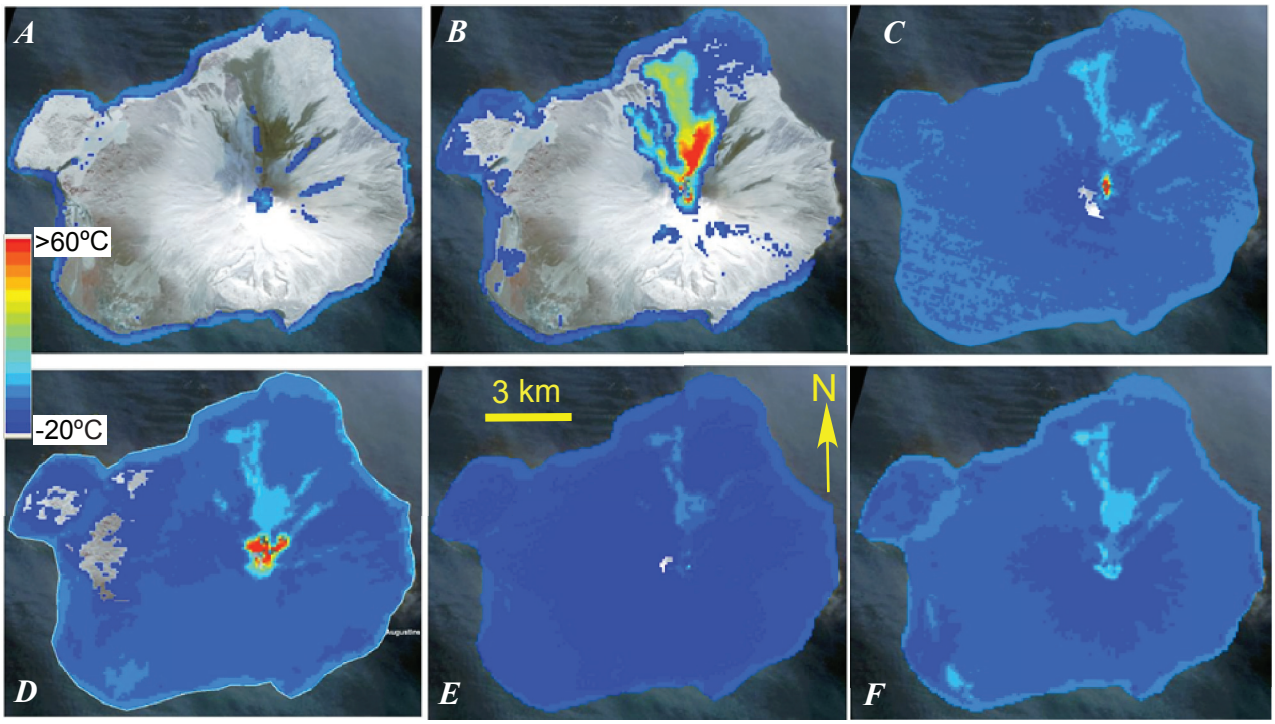

Figure 3. Advanced Spaceborne Thermal Emission and Reflection Radiometer (ASTER) pixel-integrated thermal infrared (TIR) temperatures higher than −20ºC on Augustine Volcano acquired between January 24 and May 6, 2006, showing the progression from heating of summit, through emplacement of initial pyroclastic-flow deposits after explosions in late January and early February, to effusion of first lava dome and subsequent flows as well as the gradual cooling of these volcanic deposits over time. *A*, 22:44:25 AKST January 24, 2006. *B*, 22:50:44 AKST January 31, 2006. *C*, 12:37:03 AKST February 22, 2006. *D*, 22:45:18 AKST March 13, 2006. *E*, 22:51:30 AKST April 5, 2006. F, 22:45:16 AKST May 17, 2006. Temperature data overlain on February 22, 2006, daytime ASTER visible and near-infrared (VNIR) image are visible in some images where temperatures below −20ºC were masked. North is at top of each image.

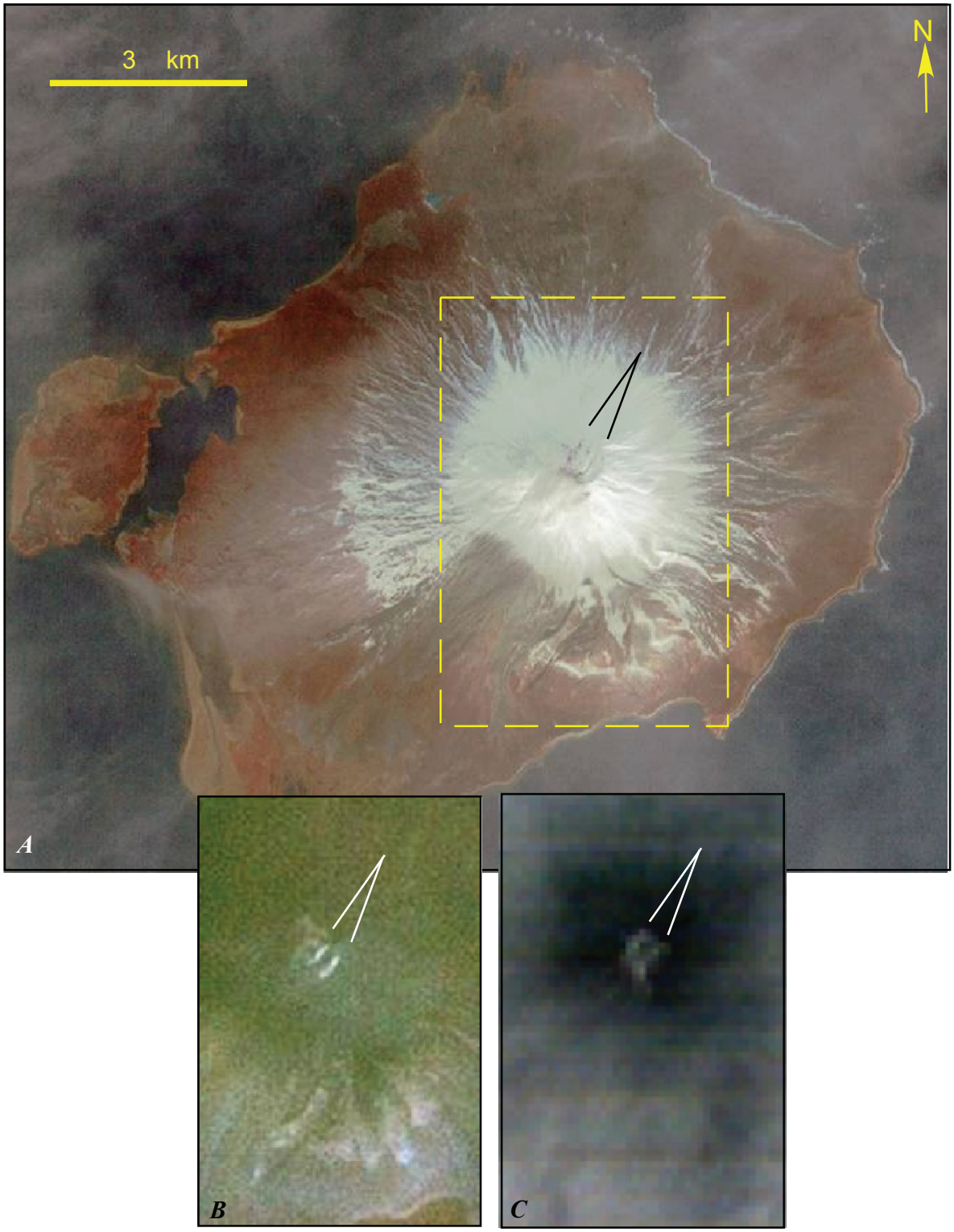

Figure 4. Partly cloudy Advanced Spaceborne Thermal Emission and Reflection Radiometer (ASTER) daytime data of Augustine Island acquired at 1235 AKST on December 20, 2005, which was only ASTER image acquired during precursory phase in late 2005 that was not completely obscured by clouds. *A*, 15 m visible and near-infrared (VNIR) image with channels 3,2,1 in R,G,B, respectively, showing the linear snow-free areas. Dashed yellow rectangle shows location of image subsets in *B* and *C*. *B*, Shortwave infrared (SWIR) image showing bright features trending same direction, likely from solar reflection off steam emanating from new fractures. *C*, Though partially obscured by thin clouds, thermal infrared (TIR) image showing elevated temperatures at the summit relative to summit temperatures in previous ASTER TIR winter observations.

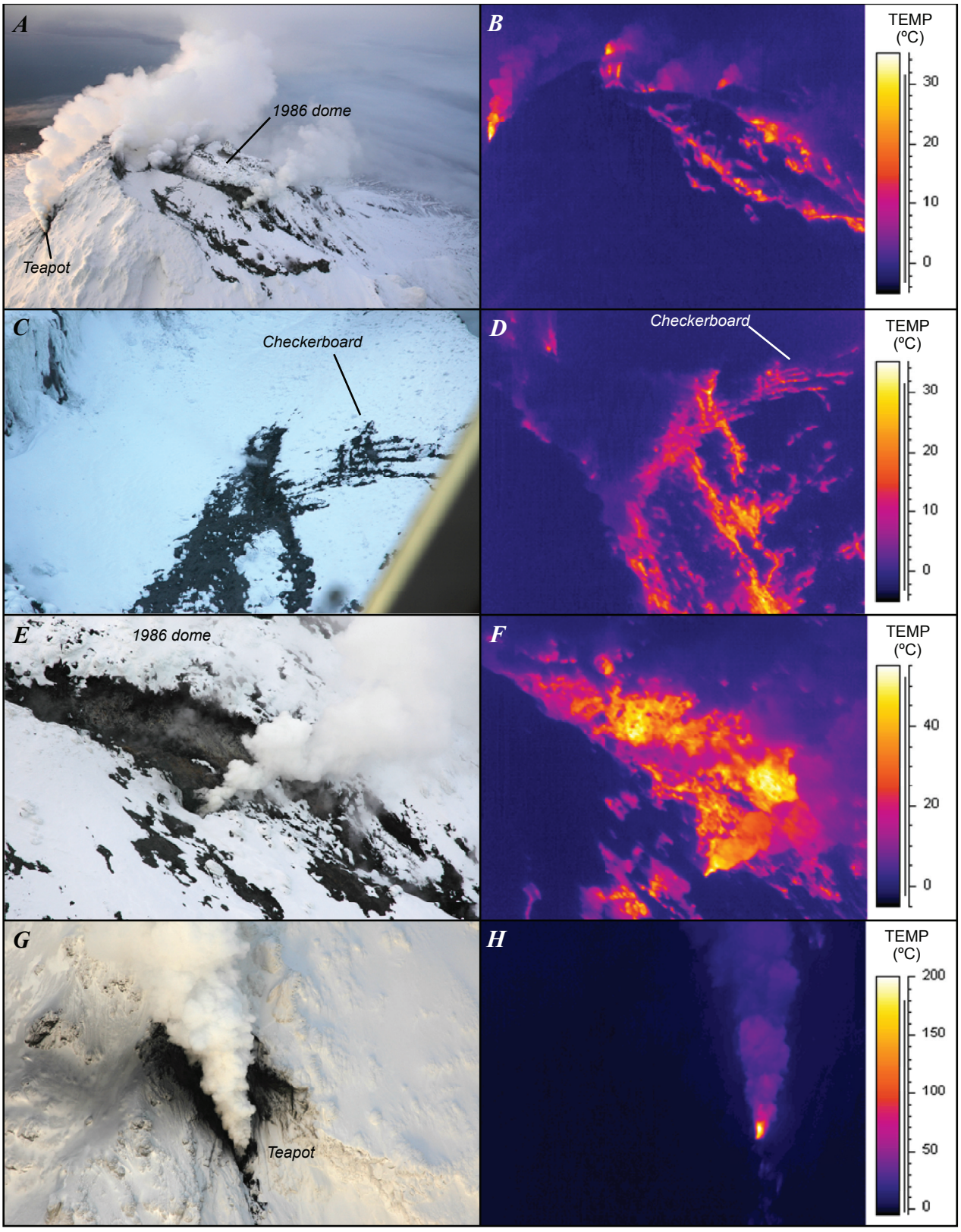

Figure 5. Photographs and thermal infrared (TIR) images of Augustine Volcano acquired during first Forward Looking Infrared Radiometer (FLIR) overflight on December 22, 2005, starting at 1509 AKST. *A,B*, Summit overview. View westward. *C,D*, "Checkerboard" pattern of snow-free fractures east of 1986 dome. *E,F*, New fumarole near edge of 1986 dome. View westward. *G,H*, Vigorously venting "teapot" fumarole on south flank.

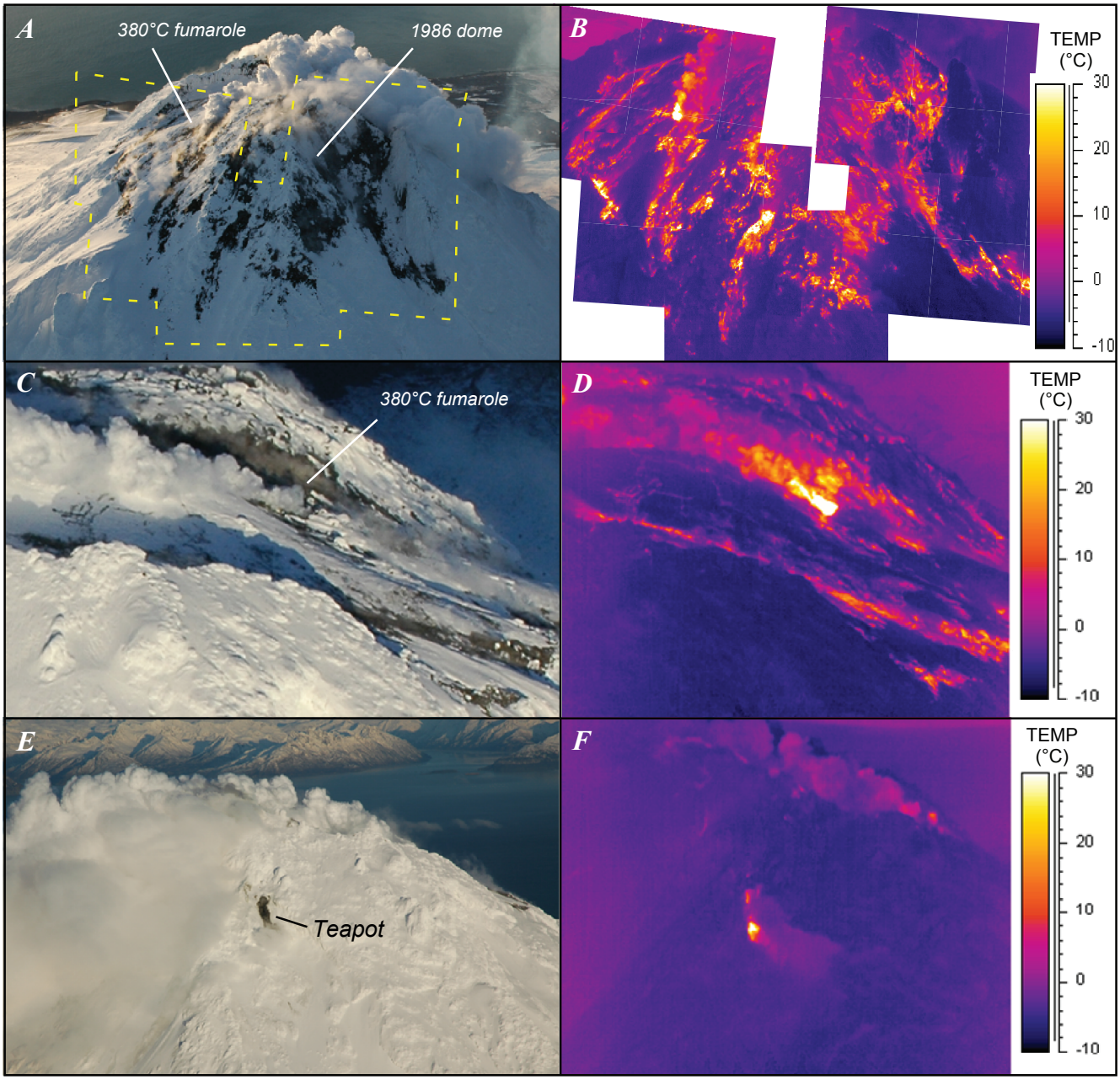

Figure 6. Photographs and thermal infrared (TIR) images of 1986 lava dome and upper flanks of Augustine Volcano acquired during Forward Looking Infrared Radiometer (FLIR) overflight on January 4, 2006. *A,B*, New warm snow-free areas extending from summit. Dashed yellow outline indicates approximate location of FLIR image mosaic shown in figure 6B. View westward. *C,D*, New fumarole along 1986 dome. View westward. *E,F*, Cooler, "Teapot" fumarole now showing only a thin steam plume. View northward.

Explosive Phase

Two explosions on the morning of January 11, 2006, heralded the beginning of the eruption's explosive phase. The explosions sent ash to 9 km above sea level (asl), but fall deposits appeared to lack juvenile material (see Wallace and others, this volume), and the explosions yielded no hot pyroclastic deposits on the island (see Coombs and others, this volume), suggesting that these explosions may have been primarily gas-release events. After about 48 hours of relative quiescence, seven more explosions on January 13 and 14 produced juvenile ash-rich clouds that rose to 14 km asl (Bailey and others, this volume; Wallace and others, this volume), hot pyroclastic flows, and secondary lahars and mixed avalanches, which were emplaced on most slopes of the volcano (see Coombs and others, this volume). Further explosions occurred on January 17, 27, and 28. A particularly explosive event on January 27 is believed to have emplaced the largest single pyroclastic-flow deposit of the entire eruption on the island's north flank (see Coombs and others, this volume). This deposit, known as the Rocky Point pyroclastic flow, approximately 4.8 km long and 17 million m^3 in volume, overran a small pond near its toe.

On January 12, 2006, 1 day after the first explosions, a FLIR helicopter mission observed that steam and ash emissions continued to reach a height of approximately 2,500 m asl and were moving southward (figs. 7*A*, 7*B*). Ash emissions waxed and waned during the time of the overflight, and a vigorous gas and ash plume emitting from a new vent, just south of the spine in the 1986 dome, was documented (figs. 7*C*, 7*D*). The maximum observed FLIR-derived brightness temperature was >275ºC, which was likely a minimum because the actual temperature exceeded the low gain setting on the FLIR. Further attempts to image this feature at a lower gain setting were unsuccessful because the vent was obscured by steam and ash emissions, which also obscured many of the elevated thermal regions visible in previous surveys, making them especially difficult to identify in images acquired from that day. Temperatures on the north face of the 1986 dome ranged from 20 to 40ºC, similar in intensity to the previous survey on January 4. Also, much less steam was observed in the south moat than during previous overflights. Drumbeat earthquakes (see Lalla

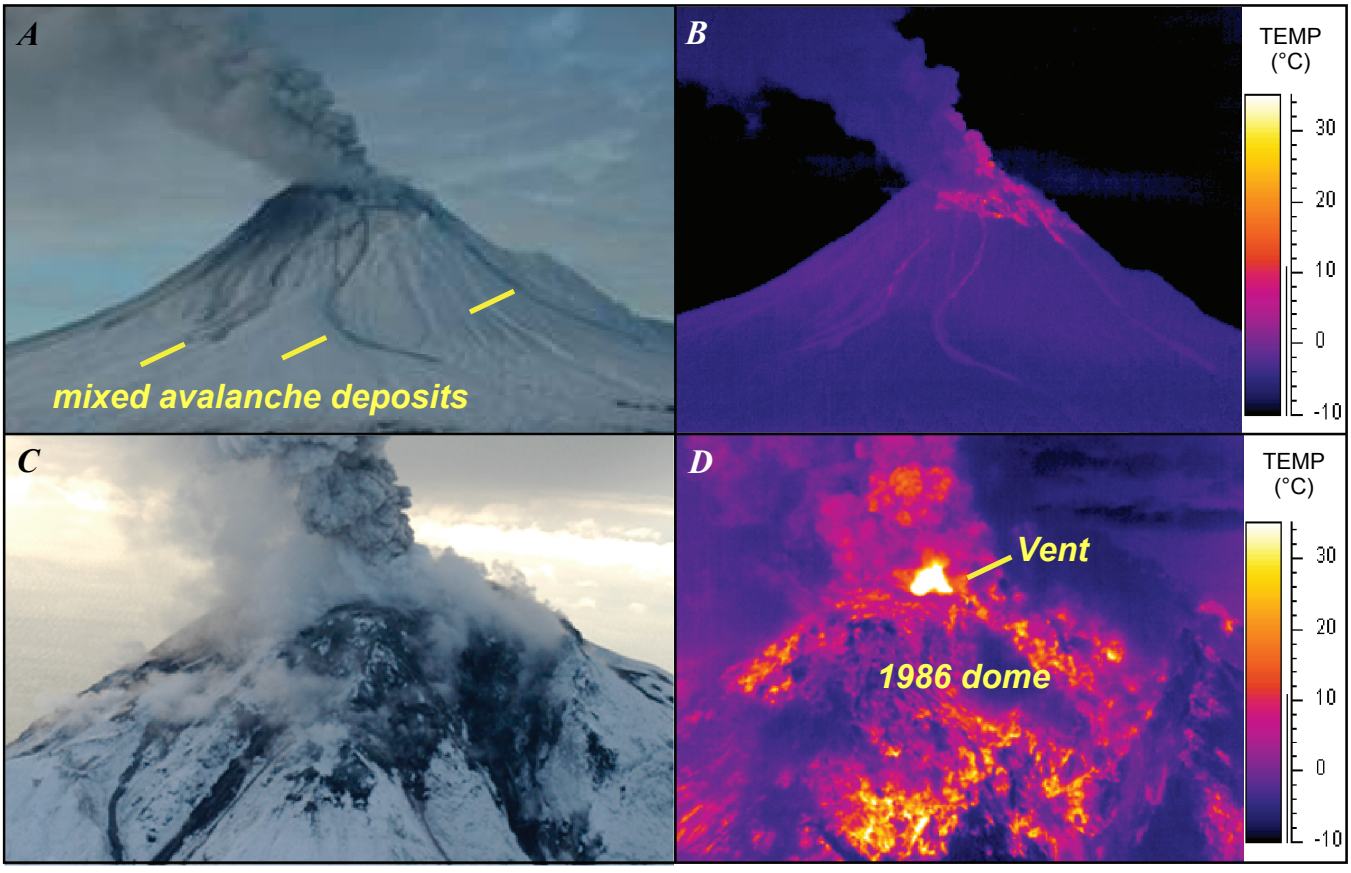

Figure 7. Photographs and thermal infrared (TIR) images of Augustine Volcano acquired during Forward Looking Infrared Radiometer (FLIR) overflight on January 12, 2006, starting at 1204 AKST. *A*,*B*, Gas and ash column venting from summit. Mixed avalanche deposits from explosions 1 and 2 on January 11, 2006, are visible on east flank. View northward. *C*,*D*, New vent (>275ºC) at top of 1986 dome. View southward.

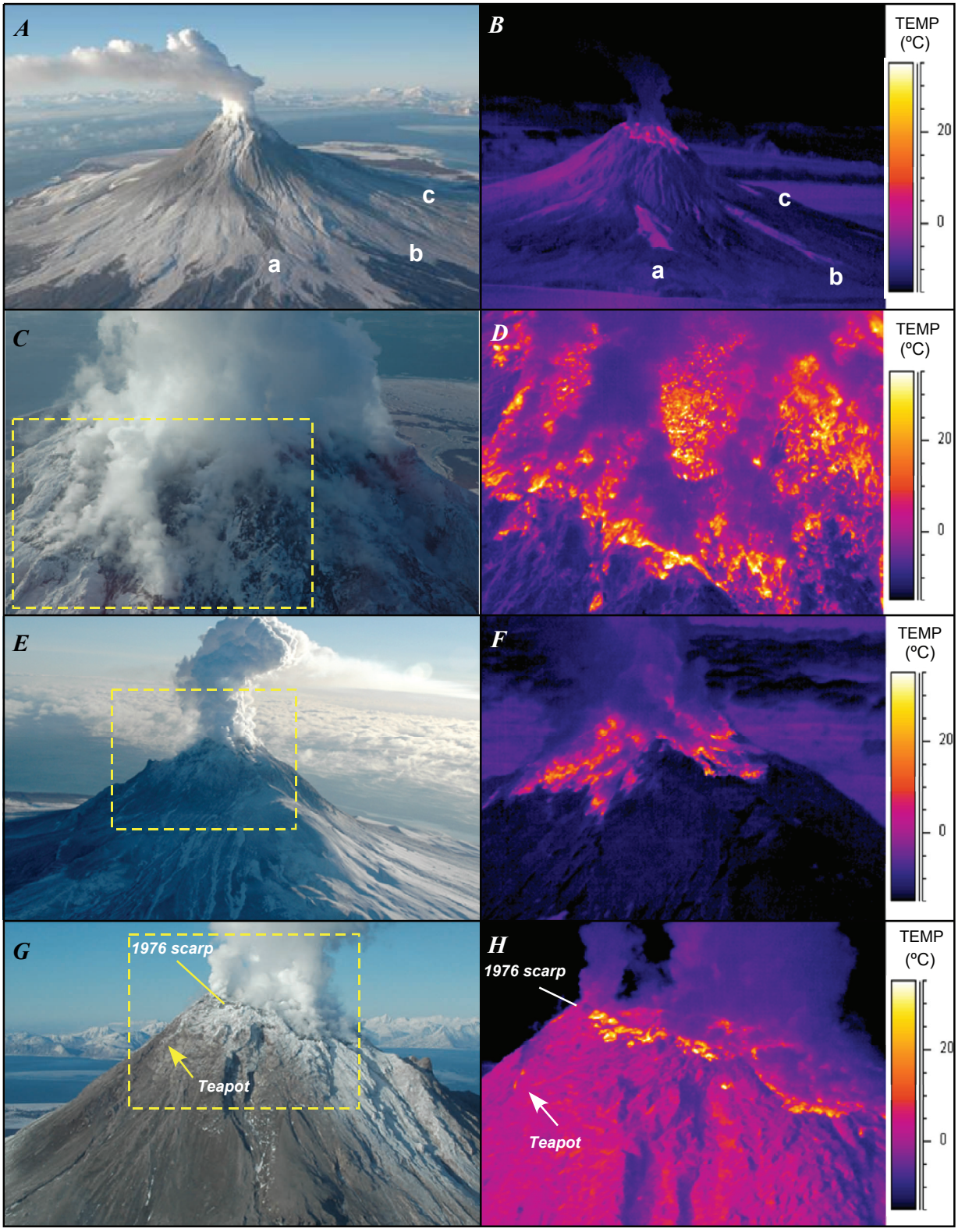

Figure 8. Photographs and thermal infrared (TIR) images of Augustine Volcano acquired during Forward Looking Infrared Radiometer (FLIR) overflight on January 24, 2006, starting at 1229 AKST. Dashed yellow boxes in *C*, *E*, and *G* indicate approximate locations of corresponding FLIR images to right. *A*,*B*, Cooling pyroclastic flows (a–c). View westward. *C*,*D*, Close-up of summit. View southwestward. *E*,*F*, Warming summit areas. View eastward. *G*,*H*, 1976 scarp at summit and "teapot" fumarole showing elevated temperatures. View westward.

and Power, this volume) and cessation of summit deformation (see Cervelli and others, this volume) suggest that lava effusion may have occurred on January 12. Saturated FLIR temperatures >275ºC were measured at the vent area through heavy steam and ash emissions, suggesting that new lava was likely present at or near the vent.

After the explosions on January 13, 14, and 17, 2006, photographs and FLIR images from January 24, showed no sign of magmatic temperatures at the summit. Cooling pyroclastic-flow deposits were observed on the east and north flanks, with surface temperatures ranging from 0 to 5ºC and a few large hot blocks, with temperatures of 30 to 40ºC (figs. 8*A*, 8*B*) were also visible. A maximum temperature of about 140ºC was observed near the new summit vent during brief views through the steam plume (figs. 8*C*, 8*D*). Steam plumes obscured much of the summit and were cold (figs. 8*E*–8*H*). Most of the summit region consisted of warm rubble, with temperatures ranging from 20 to 40ºC.

Nighttime ASTER TIR images from January 24, 2006, shows elevated summit temperatures and warm pyroclastic-flow deposits from the January 13–17 explosions on the northeast flanks (fig. 3*A*).

Continuous Phase

At about 1430 AKST on January 28, the volcano entered a period of more nearly continuous eruptive activity characterized by nearly constant ash-rich plume emissions to average heights of 3,600 m asl or less, as recorded by satellite data and radar (see Bailey and others, this volume). Occasional larger seismic signals, assumed to represent larger explosions, were associated with larger ash clouds up to 4,600 to 7,600 m asl. Subsequent observations showed that thick fans of pyroclastic material were deposited north and northeast of the summit during this period (see Coombs and others, this volume). This phase has been interpreted as the result of rapid effusion of lava at the summit, accompanied by nearly instantaneous collapse of parts of the growing lava dome to form numerous block-and-ash flows (see Coombs and others, this volume). Activity waned on February 3, and lower effusion rates produced a new lava dome and flow during the next week. Poor weather and low-lying ash obscured visual and satellite views during much of this period.

During the night of January 31, 2006, the ASTER URP system imaged an ash- and SO_2-rich plume and several large, hot pyroclastic-flow deposits on the volcano's north flank, including the Rocky Point pyroclastic flow that extends nearly to the north shoreline (fig. 3*B*). The 90-m ASTER TIR data show subtle temperature differences between the cooler distal ends of the pyroclastic-flow deposits and the warmer proximal areas. These temperature differences were likely controlled by both the age (hours) and thickness of the deposits. Multispectral TIR data also provide the means to identify silicate ash, ice, and SO_2 components in the plumes. ASTER SWIR (30 m) data from the same period show a ~700-m by 300-m region of hot pixels centered at the summit dome, with a maximum brightness temperature of 619°C.

A FLIR overflight on February 8, 2006, revealed several areas of cooling pyroclastic-flow deposits (fig. 9), the most extensive of which were in the northeast to northwest sectors. Smaller flows were deposited on the east flank (toward the Mound site), and a very small flow was observed on the southwest flank. Most of the pyroclastic-flow deposits had temperatures of 10–25°C, with numerous hotter large blocks (presumably dome fragments) with maximum temperatures >120°C. Pyroclastic-flow-deposit locations on the north and northwest flanks matched quite well with the warm features on the flanks observed in the nighttime TIR ASTER image of January 31 (fig. 3B). FLIR images of the summit were extremely difficult to acquire because of persistent steaming and cloud cover (fig. 9*A*). The maximum observed summit temperature of a contiguous area centered over the 1986 dome was ~50°C (fig. 9*B*); given the thick cloud cover, the actual temperature would have been much higher. Occasional photograph views through the steam and cloud showed a large black feature at the summit that was likely a new dome.

Eruptive Pause

From about February 10 through March 3, 2006, lava dome and flow effusion paused or at least slowed significantly (see Coombs and others, this volume). Limited thermal and visible views show little, if any, growth of the lava dome and flows during this period. FLIR and ASTER data spanning February 20–24 show a hot summit dome and rockfall deposits down the north flank and gradual cooling of the pyroclastic-flow deposits (figs. 3*C*, 10). FLIR images acquired on both February 20 and 24 detected maximum temperatures of 300°C at the edge of and below the active lava flow extending northward from the summit dome. The average surface temperature in mostly clear views of the summit dome was 40°C, whereas the average surface temperature of flows beneath the dome was 100°C. A wide area of steaming, bare rock surrounded the crater (figs. 10*C*, 10*E*), extending tens of meters down the flanks outside the 1976 crater (figs. 10*E*, 10*F*). The FLIR images, scaled for distance and pixel size, show that the warm north part of the dome was about 100 m wide and 115 m high. The slope distance from the top of the dome to the base of the 85-m-wide flow was approximately 390 m (275 m in plan view). Hot-rock deposits were also observed below the dome and along the lava flow in three distinct channels on the north flank (fig. 2*C*, 2*D*). The surfaces of the pyroclastic-flow deposits from late January had cooled to ~5°C.

Effusive Phase

After the apparent pause in eruptive activity throughout the second half of February, Augustine Volcano resumed

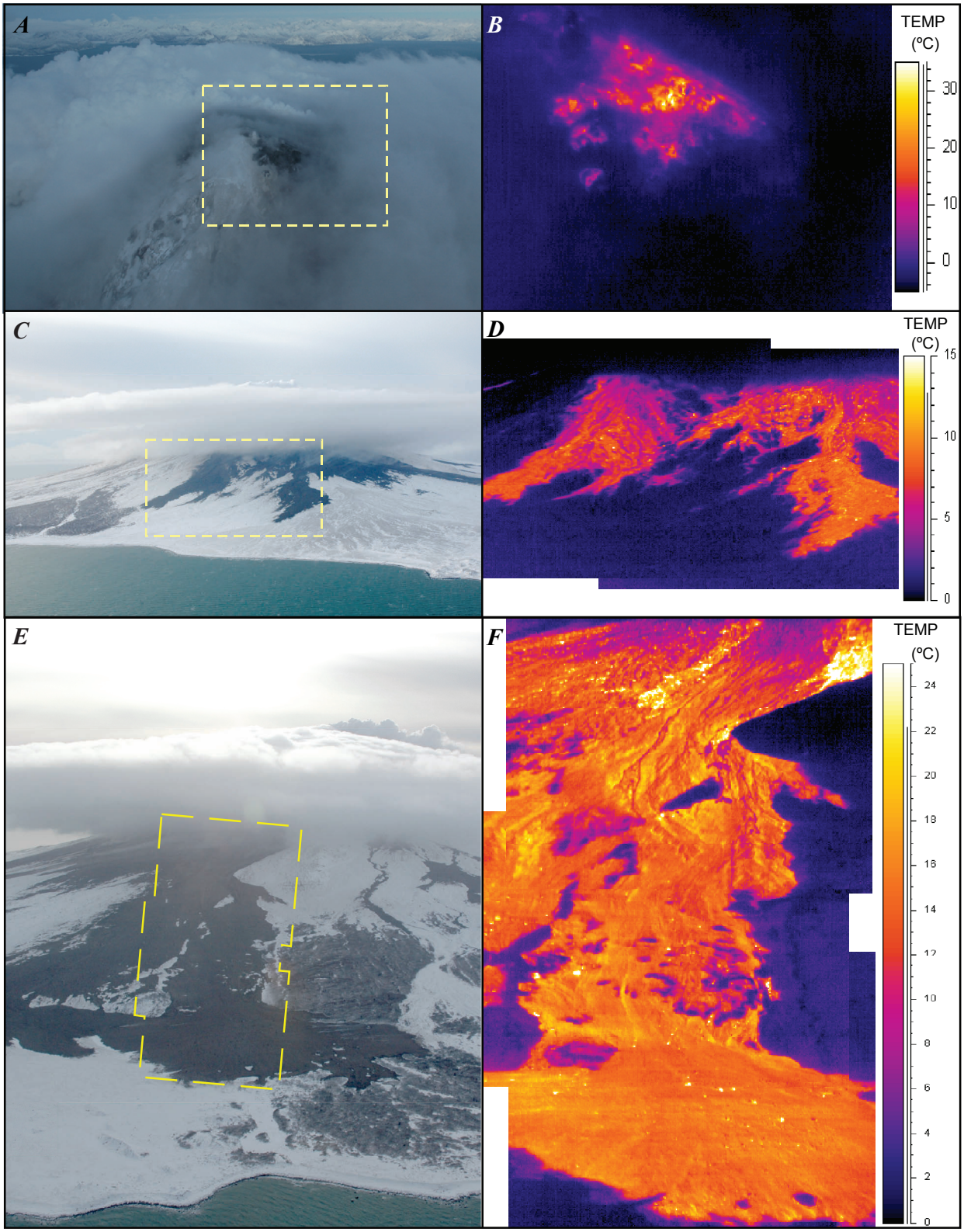

Figure 9. Photographs and thermal infrared (TIR) images of Augustine Volcano acquired during Forward Looking Infrared Radiometer (FLIR) overflight on February 8, 2006, starting at 1149 AKST. Dashed yellow boxes indicate approximate locations of corresponding FLIR image mosaics to right. *A*,*B*, Summit through thicker clouds. Dark, warm area might be obscured view of a new dome. View westward. *C*,*D*, Pyroclastic-flow deposits on northeast flank. View southwestward. *E*,*F*, Rocky Point pyroclastic-flow deposit. View southeastward.

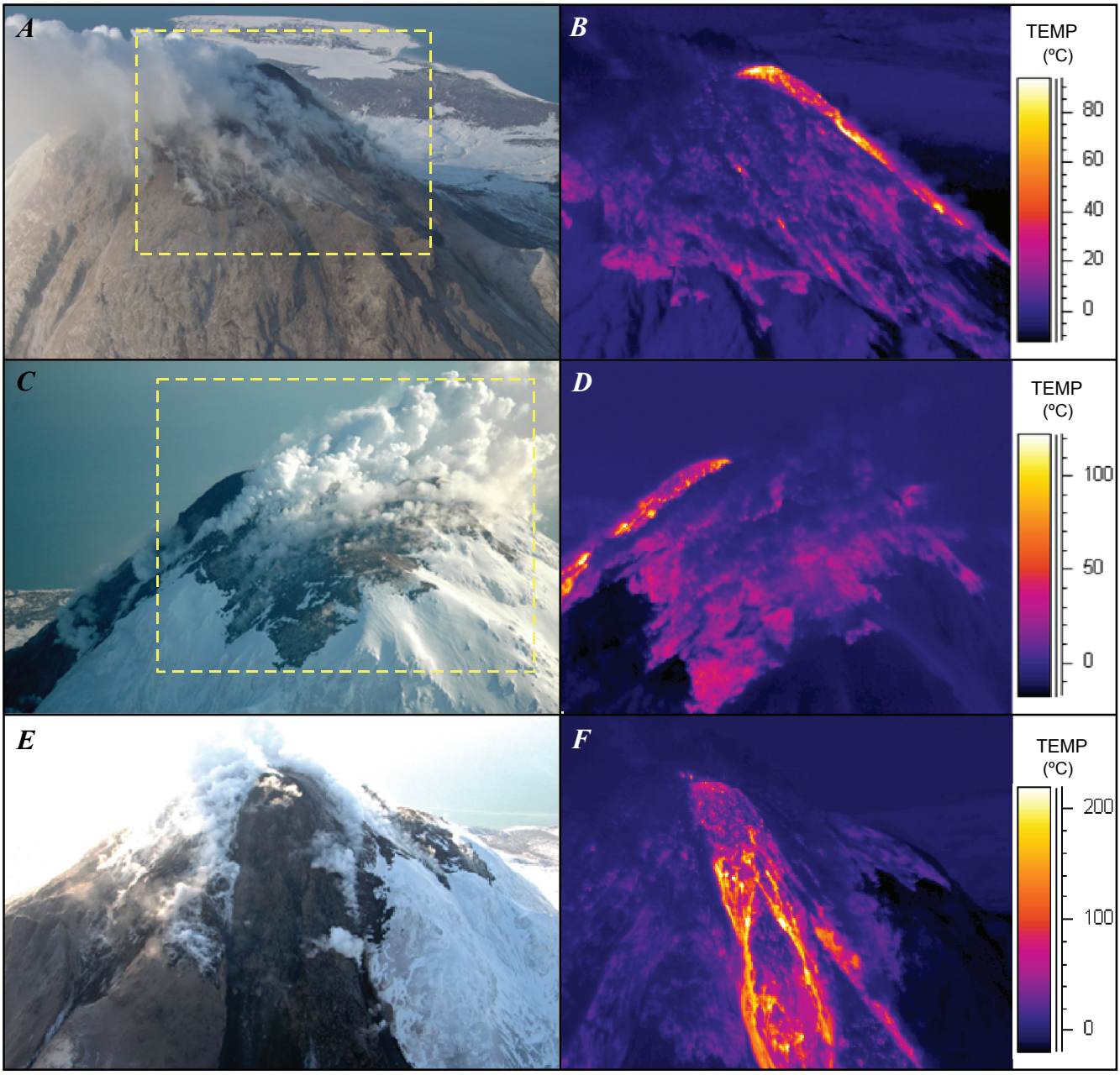

Figure 10. Photographs and thermal infrared (TIR) images of Augustine Volcano acquired during Forward Looking Infrared Radiometer (FLIR) overflight on February 24, 2006. Dashed yellow boxes in *A* and *C* indicate approximate locations of corresponding FLIR images to right. *A*,*B*, New summit lava dome, north lava flow, and hot rubble below flow, showing an expanded area of warm and steaming rock. View westward. *C*,*D*, Expanded area of warm and steaming rock at summit. View eastward. *E*,*F*, North lava flow and lava dome. View southward.

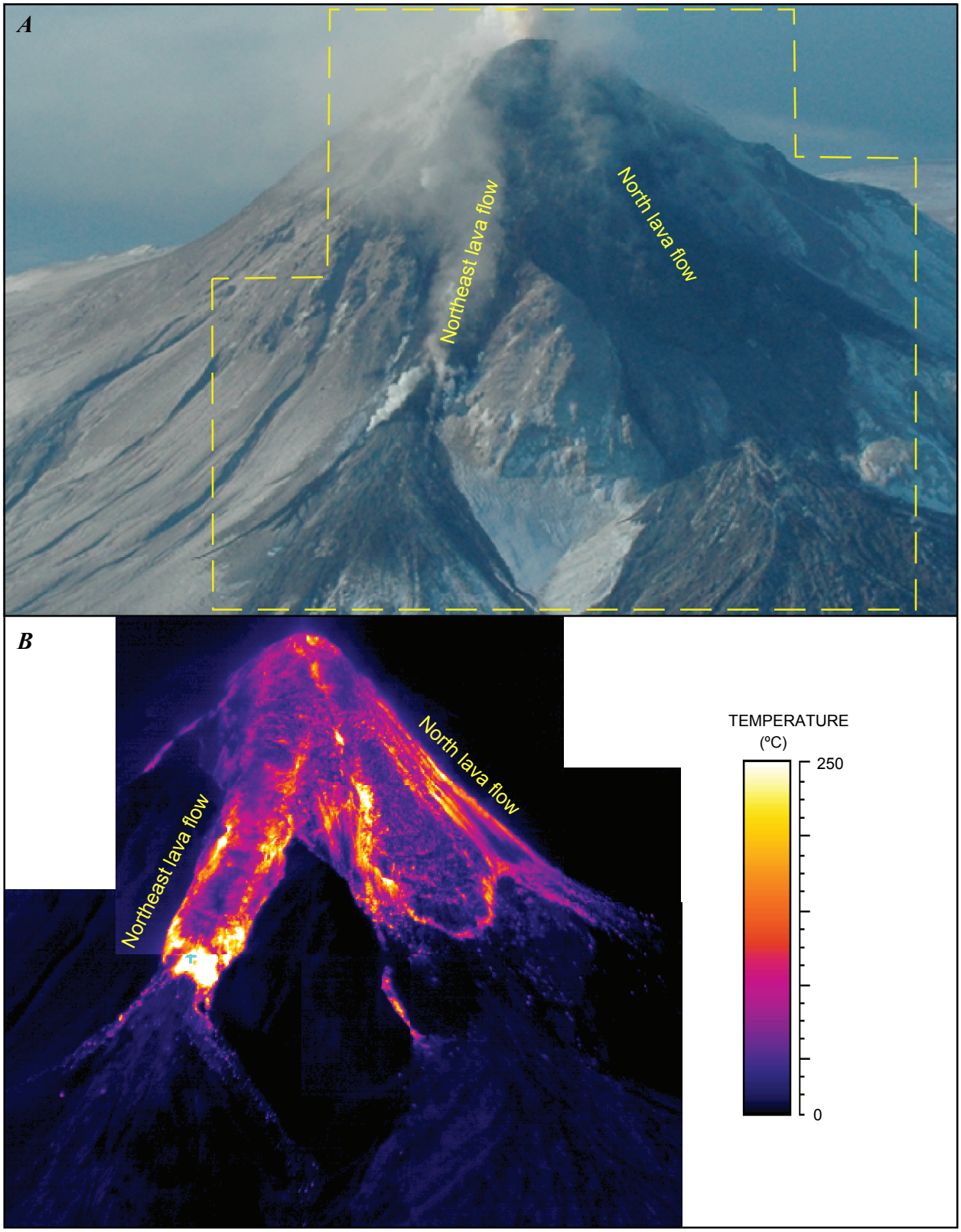

Figure 11. Photographs and thermal infrared (TIR) images of Augustine Volcano acquired 0959 AKST March 10, 2006, during Forward Looking Infrared Radiometer (FLIR) overflight. *A*,*B*, New summit lava dome and northeast and north lava flows. Summit and flows are partly obscured by dust and hot gas from frequent rockfalls from advancing flows, which are also visible in FLIR mosaic image. View southwestward.

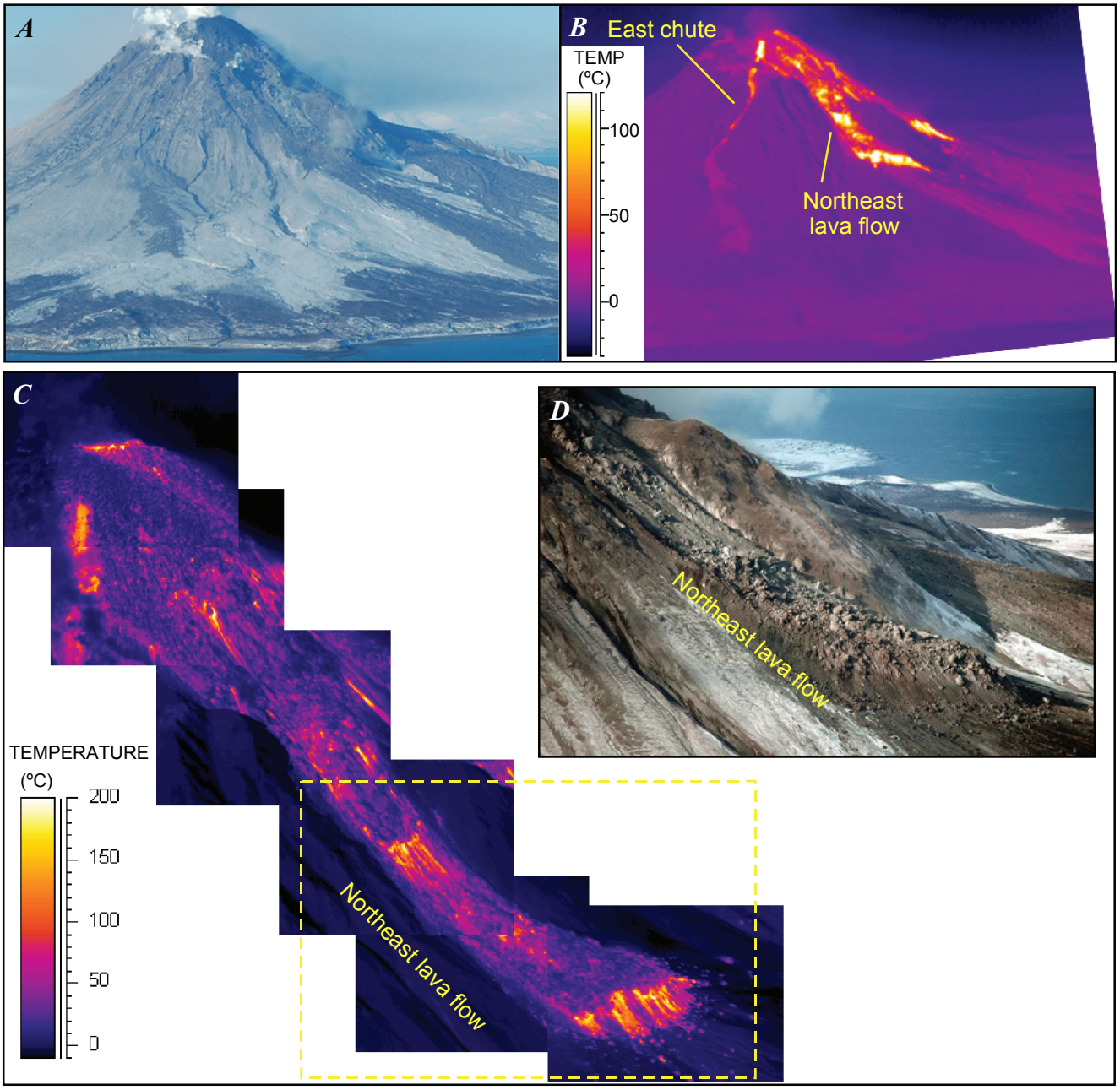

Figure 12. Photographs and thermal infrared (TIR) images of Augustine Volcano acquired during Forward Looking Infrared Radiometer (FLIR) overflight on March 15, 2006, starting at 0953 AKST. *A*,*B*, Entire volcano, with hot lava flows and small block-and-ash deposits extending down east chute below new summit lava dome. View westward. *C*,*D*, Mosaic of 6 close-up FLIR images of northeast lava flow and lava dome. Dashed yellow box indicates approximate location of figure 12*D*. View southeastward.

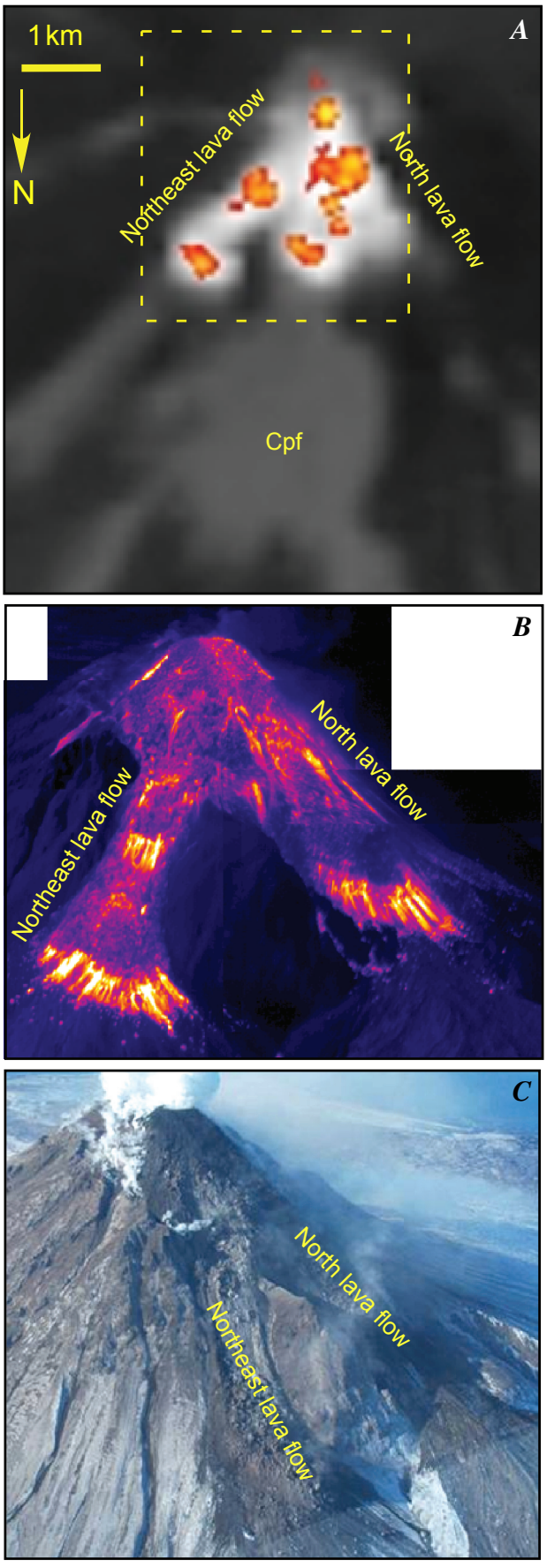

activity in March with the effusion of a larger summit dome, renewed growth of the north lava flow, and formation of a new lava flow confined to an erosional channel on the northeast side of the volcano, all accompanied by vigorous block-and-ash flows. This phase likely began on March 3 with an increase in the number of rockfall signals detected seismically, followed by a series of small explosions on March 4 (see Coombs and others, this volume; Power and Lalla, this volume). From March 8 to 16, seismic stations on the island recorded strong drumbeat earthquakes, indicative of lava effusion (see Power and Lalla, this volume), and incandescence was observed in Homer (see Sentman and others, this volume) and recorded by the Burr Point time-lapse camera (see Coombs and others, this volume). FLIR data acquired on March 10 and 15 provide some of the best information about growth of the new dome and flows (figs. 11, 12).

FLIR images from March 10, 2006, clearly show the larger dome and the two lava flows on the upper north and northeast flanks (figs. 2*E*, 2*F*, 11). A maximum temperature of 700°C was measured at the toe of the northeast lava flow, the highest temperature measured during the 2006 eruption. Mostly clear views of the summit dome revealed average surface temperatures of ~40°C; the average surface temperature of flows downslope from the dome was 100°C. The wide area of steaming, bare rock surrounding the crater that was observed in February persisted. The pyroclastic-flow deposits emplaced in late January had surface temperatures averaging 4°C, but were still steaming over the area of the now-buried pond.

On March 15, the north and northeast lava flows had both advanced and thickened since March 10. On the basis of scaled FLIR images from Burr Point (fig. 2*H*), the northeast flow advanced approximately 140 m to a total length of 930 m as measured from the base of the summit dome.

Figure 13. Comparison of multiscale, multispectral data of Augustine Volcano summit acquired March 13–15, 2006. *A*, March 13, 2006, Advanced Spaceborne Thermal Emission and Reflection Radiometer (ASTER) nighttime thermal infrared (TIR) image. *B*, Oblique airborne Forward Looking Infrared Radiometer (FLIR) image acquired 1.5 days later on March 15. *C*, Photograph taken at same time as FLIR image. ASTER image shows high temperature shortwave infrared (SWIR) (30 m) pixels in color over grayscale TIR (90 m) pixels. Map view in ASTER image is rotated with north at bottom to better match views in oblique photographs. Yellow dashed rectangle outlines approximate area of *B*. Combined TIR-SWIR ASTER image highlights benefit of having both datasets, with TIR image defining outline of active lava flows and SWIR image highlighting areas of exposed lava at surface. This SWIR image also reveals that both flows have zones of freshly exposed lava in areas of high extension-strain rate, as well as at summit and toes of flows.

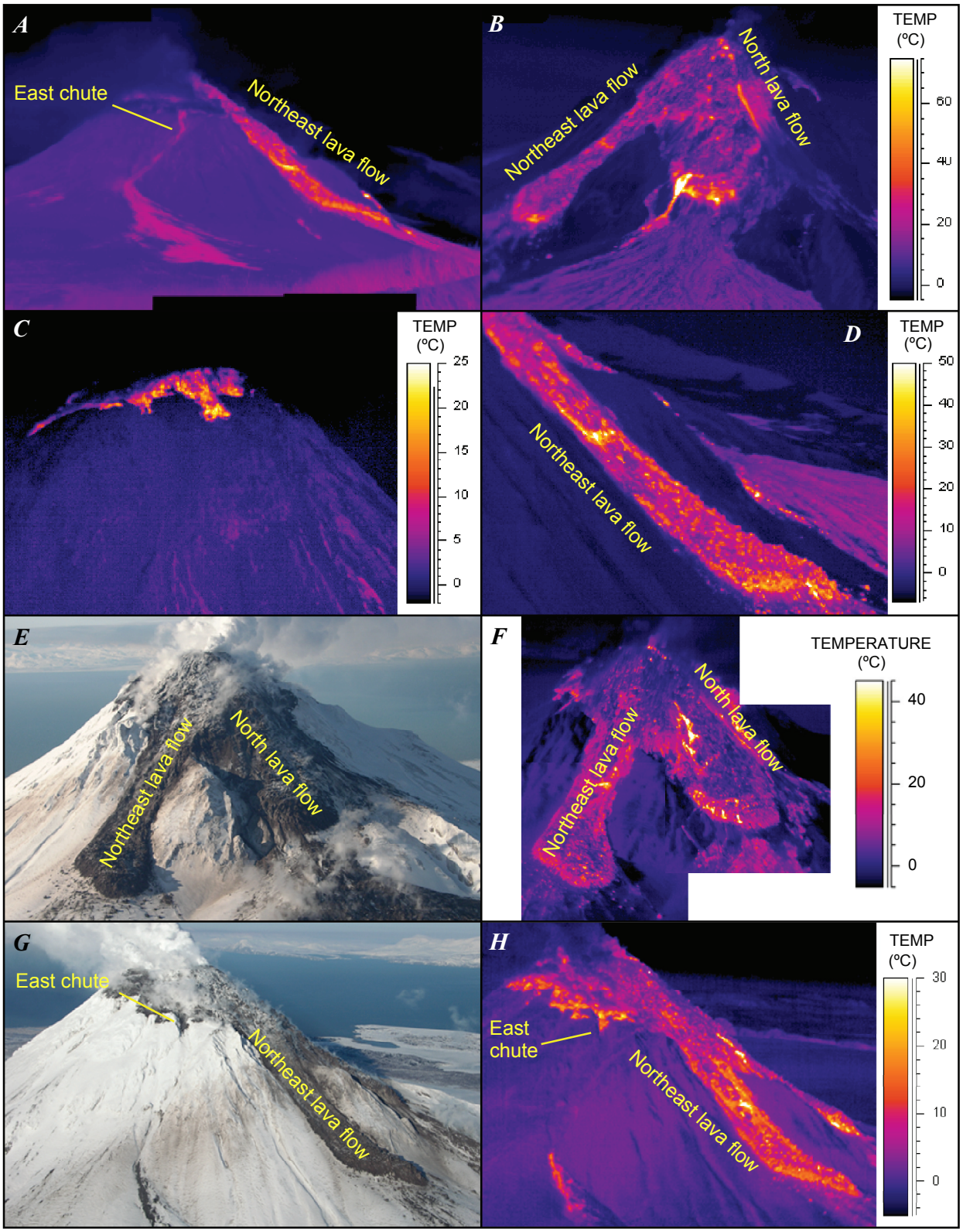

Figure 14. Photographs and thermal infrared (TIR) images of Augustine Volcano acquired during Forward Looking Infrared Radiometer (FLIR) overflights on March 26, 2006 (*A–D*), and April 6, 2006 (*E–H*). *A*, Northeast lava flow and warm, though apparently inactive, east chute (see fig. 12*C*). View westward. *B*, Northeast and north lava flows. Note active spalling along east side of north lava flow. View southward. *C*, Warm surface of summit scarp. View northeastward. *D*, Northeast lava flow. View westward. *E*,*F*, Lava flows. View southward. *G*,*H*, Northeast lava flow and east chute. View westward.

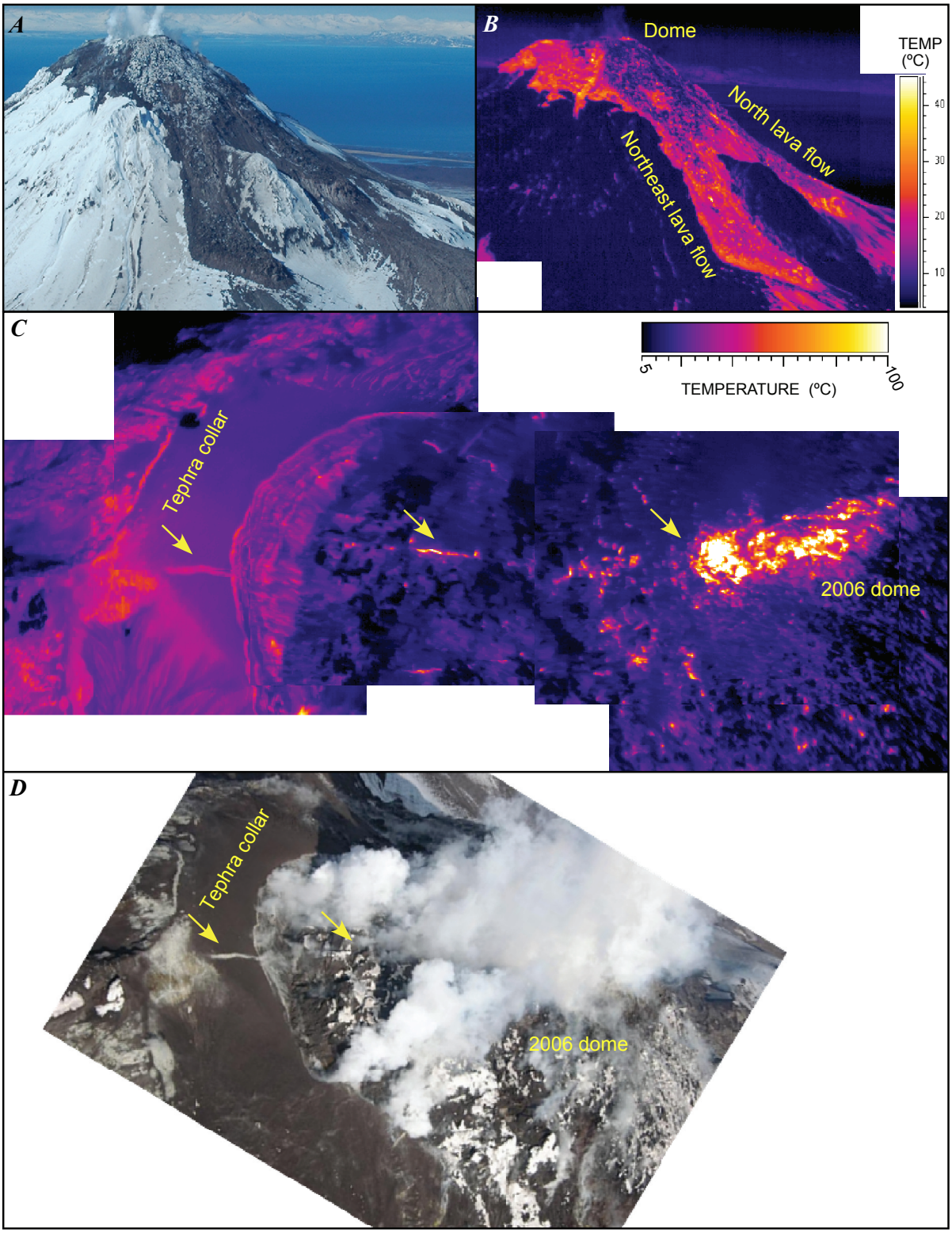

Figure 15. Photographs and thermal infrared (TIR) images of Augustine Volcano acquired during Forward Looking Infrared Radiometer (FLIR) overflight on May 13, 2006. *A*,*B*, Northeast and north lava flows, summit lava dome, and warm deposits on south side of summit. New dome rock is partly covered by a combination of snow, ice, and precipitates, whereas tephra deposits adjacent to dome remain snow free. View southward. *C*,*D*, Summit lava dome and tephra collar. Note elongate zone of high temperatures on dome and hot fractures extending southward from dome (arrows). South is to the left in both figures.

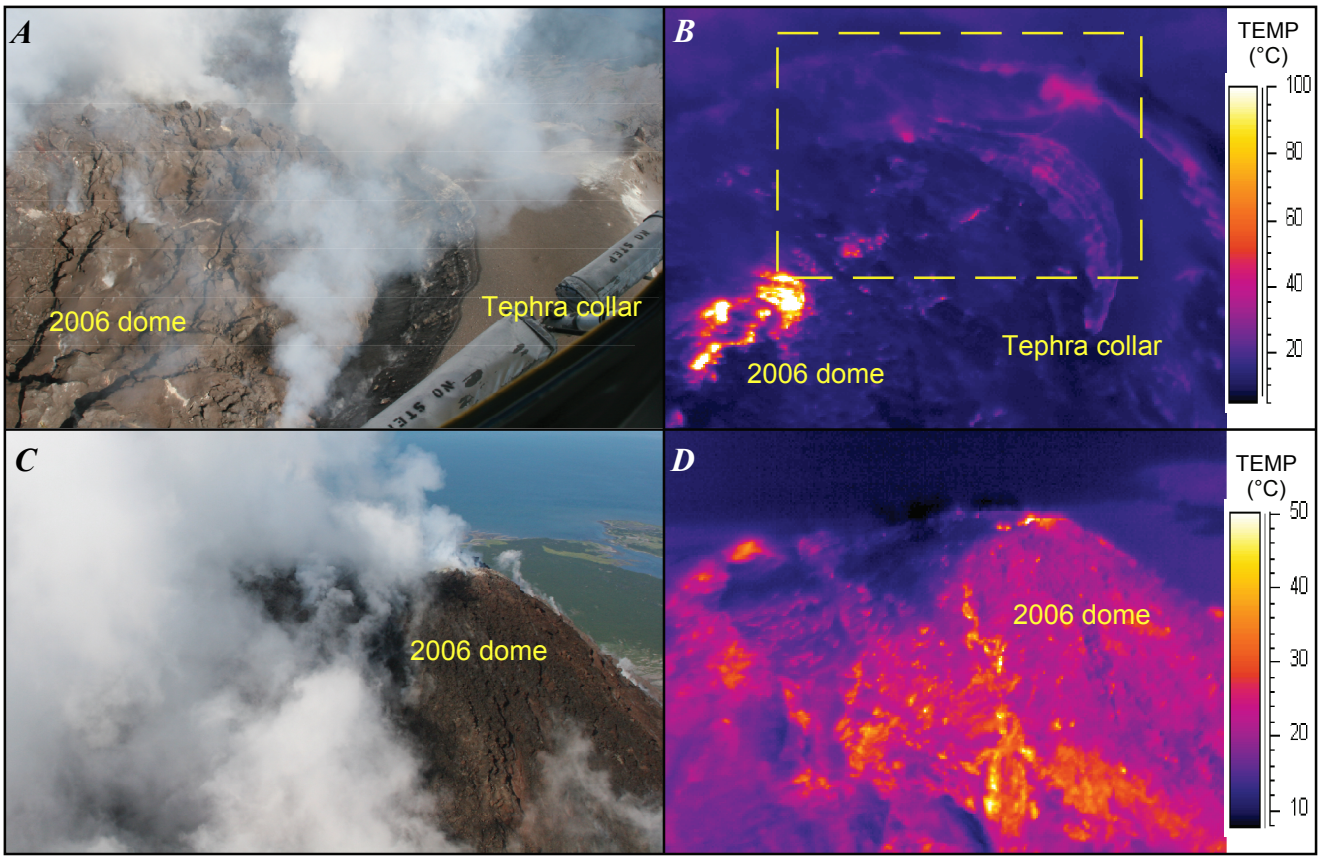

Figure 16. Comparisons between photographs and thermal infrared (TIR) images of Augustine Volcano acquired during final Forward Looking Infrared Radiometer (FLIR) overflight on August 7, 2006. *A–B*, Part of 2006 lava dome and 2006 tephra collar on south rim. Elongate zone of high temperatures on dome and hot fractures extending southward from dome persist. Dashed yellow box indicates approximate location of *A*. *C*,*D*, Summit lava dome, tephra collar, and remnants of east chute. View westward.

The north lava flow widened from by about 70 m to 410 m, but advanced downslope only approximately 20 m to a total length of 420 m. Most of the thermal energy was emitted from flow fronts and small windows through the rubble-covered carapace created by tensional fracturing as the flow advanced over steeper topography. This carapace was most notable on the east side of the dome, although no visible incandescence was observed anywhere along the flow edges (fig. 12*D*). Minimal rockfall activity suggested that the flows were generally advancing more slowly than on March 10. The average temperature measured on the flow and dome surfaces had decreased to ~40°C. The extent and temperatures of warm areas on the summit flanks were unchanged from March 10 and earlier.

FLIR data show the variation in temperature on the lava flow surfaces (fig. 12*E, 13B*). Both the lava flows and the dome edges have steeper areas of hotter material at the surface. The hot lava flows were observed about 34 hours before the FLIR survey by a nighttime ASTER image. The 90-m TIR image (figs. 3*D*, 13*A*) reveals the extent and temperature of the hot summit dome and flows as bright, sometimes saturated, pixels. The maximum pixel-integrated temperature extracted from ASTER 30-m SWIR (2.167 µm) radiance data was 463.9°C (fig. 13*A*).

Post Eruption

Seismic activity had dropped to pre-effusive-phase levels by March 20 (see Power and Lalla, this volume), and no new morphologic changes in the dome or lava flows were observed after March 15. Incandescence after this time was focused along the west margin of the north lava flow, where spalling and rockfalls continued to occur into May (see Coombs and others, this volume).

FLIR data from March 26 (figs. 14*A*–14*D*) showed that the average surface temperature was low, (~40°C). The lava flow fronts where fresh spalling had previously occurred had

maximum temperatures of 180°C. Viewed at close range (500 m), one summit fumarole had a maximum temperature of 221°C. The southwest side of the summit had warm areas extending a short distance downward from the summit.

On April 6 (figs. 14*E*–14*H*) the north and northeast lava flows had not advanced notably since previous observations on March 15 and 26. The flow fronts also appeared to be cooler relative to the previous surveys, with little rockfall from their fronts. The north-lava-flow front and margins appeared to be more active than those of the northeast flow. The average temperature of the flow and dome surfaces was similar to that in previous surveys in March (~40°C), and the extent and temperatures of the warm areas on summit flanks appear to be unchanged from previous surveys.

The maximum temperature of ~650°C in a fumarole at the top of the dome was considerably higher than that recorded on March 26 (220°C), possibly owing to better viewing conditions on April 6, but also reflecting changes in the vent geometry since the previous survey. Although gas measurements by McGee and others (this volume) show a gradual decrease in SO_2 flux from late March through April, day-to-day averages vary somewhat during this period. The measured April 6 average SO_2 flux (~2 kt/d) was nearly double the flux for March 22 (~1 kt/d).

A FLIR survey of Augustine Volcano on May 13, 2006 (figs. 15*A*–*15D*) showed no obvious morphologic changes to domes or flows since April. The maximum temperature of 428°C recorded at the top center of the 2006 dome was lower than that recorded on April 6 (650°C). Warm areas persisted around the summit region, unchanged from previous surveys. The north- south-trending fractures first observed on the summit in December 2005 continued to persist as linear

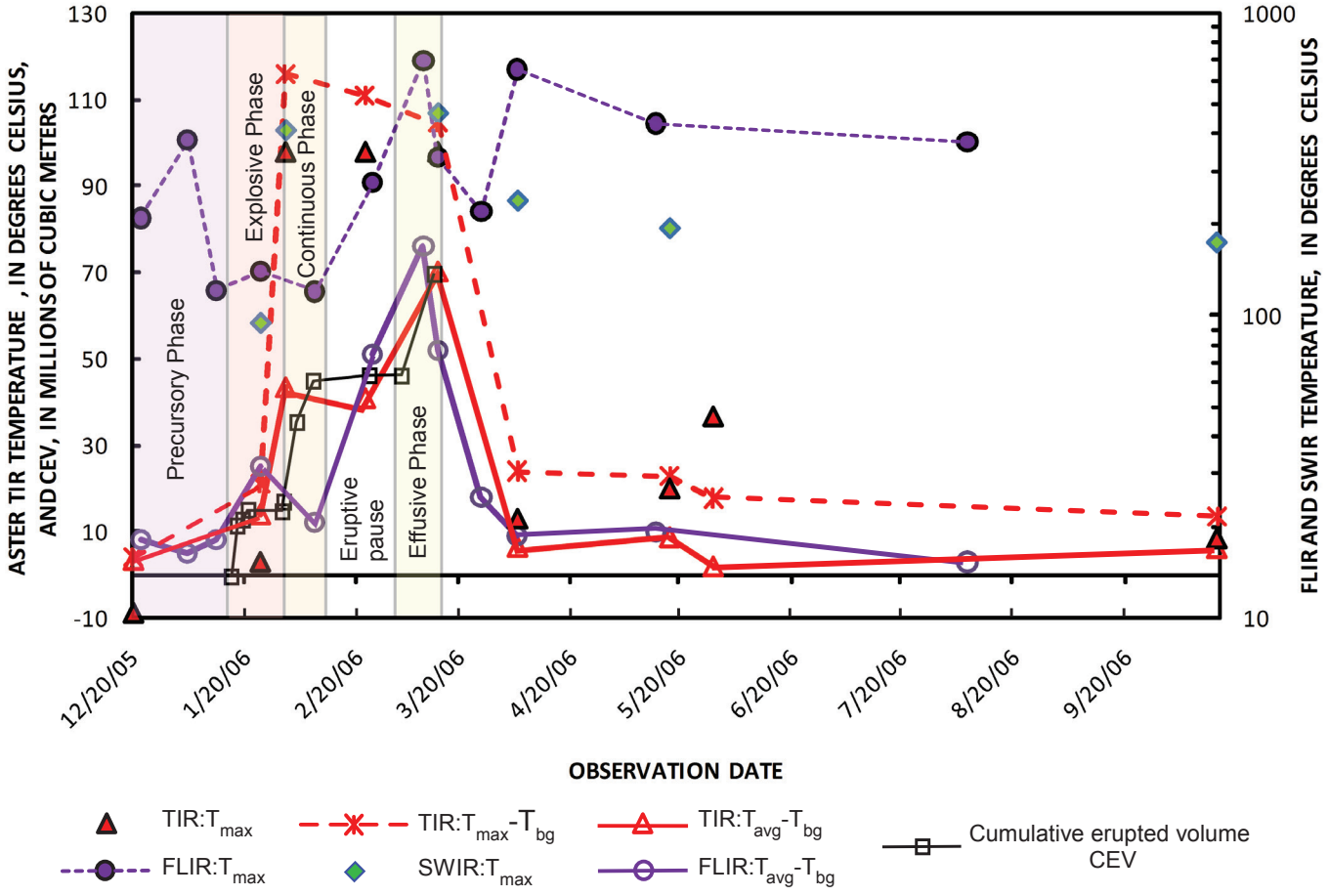

Figure 17. Advanced Spaceborne Thermal Emission and Reflection Radiometer (ASTER)- and Forward Looking Infrared Radiometer (FLIR)-derived temperatures (see tables 1, 2) and cumulative erupted volume (black squares; from Coombs and others, this volume) during each phase of 2006 eruption of Augustine Volcano versus date. Red solid triangles, maximum ASTER thermal infrared (TIR) temperatures at summit; red open triangles, ASTER TIR average lava-flow-surface temperature minus background temperature near summit elevation. Maximum ASTER TIR temperatures >100°C indicate data saturation during continuous and effusive phases. Green diamonds, maximum ASTER shortwave infrared (SWIR) brightness temperatures at summit; Purple dots, maximum temperature in multiple airborne FLIR images. Purple circles show average FLIR lava surface temperature minus FLIR background temperature.

warm areas atop the new dome and tephra collar with the same orientation.

The final FLIR survey of Augustine Volcano was conducted on August 7, 2006 (figs. 16*A–16D*). The summit lava dome surface and tephra collar had temperatures similar to those in the May survey. Corrected for background temperature, the flow surfaces had cooled ~7°C since May to ~3°C above background. FLIR data show that most of the new lava flow surfaces were barely above ambient temperature, although several areas of warm rubble had average surface temperatures of 30°C. Hot fumaroles persisted at the summit and in several parts of the new lava flows. The temperature of the 2006 summit dome fumarole was still ~370°C, and several fumaroles around the perimeter of the new flows had maximum temperatures of 150°C. The pyroclastic-flow deposits and the north and northeast lava flows were not imaged with FLIR during the final survey.

Summary and Conclusions

The combined near-real-time utilization of both airborne and satellite TIR images during the eruption of Augustine Volcano provided valuable insights into the eruption hazards and dynamics. The high-resolution TIR images documented gradual pre-eruption heating of the summit, growing pyroclastic-flow deposits, rapid temperature increases as the lava dome and flows formed, and slow cooling of the volcanic deposits after the eruption (fig. 17). These high-resolution images uniquely documented segmentation of the lava flows into hotter areas of increased flow deformation and cooler, more stable crust on the active flows.

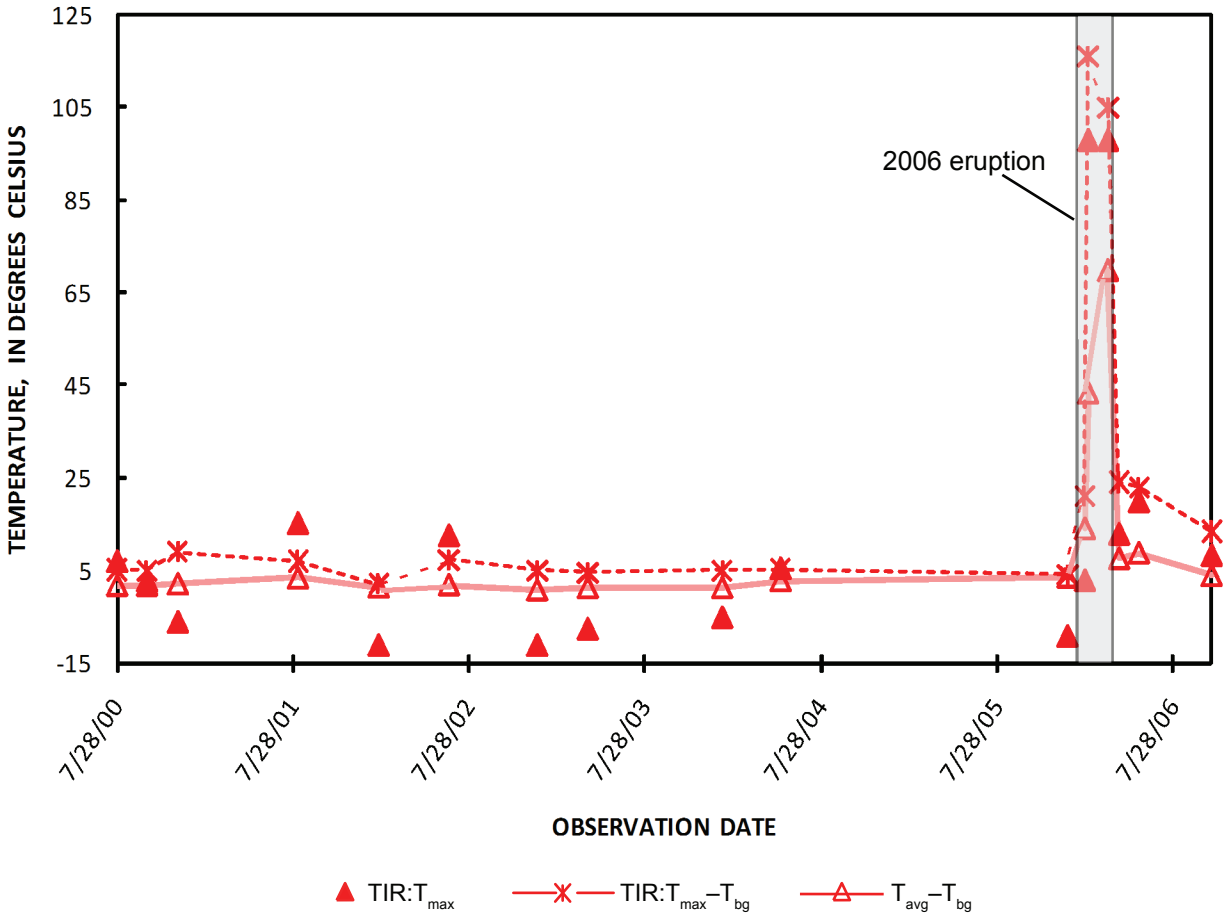

Figure 18. Advanced Spaceborne Thermal Emission and Reflection Radiometer (ASTER)-derived temperatures from July 28, 2000, to October 15, 2006. Red solid triangles, maximum ASTER thermal infrared (TIR) temperature at summit; red open triangles, average ASTER TIR surface temperature at summit minus background temperature near summit elevation; asterisks, maximum ASTER TIR temperature at summit minus background temperature near summit elevation.

The temperatures derived from FLIR and ASTER images are plotted against the cumulative erupted volume and eruptive phases (see Coombs and others, this volume) in figure 17. The widely varying maximum FLIR-derived temperatures (FLIR:T_{max}, fig. 17; table 1) for each overflight were from thermal features ranging from fumaroles at the summit during the precursory phase, through individual hot blocks in fresh pyroclastic-flow deposits during the explosive and continuous phases, to large incandescent fractures and spalling lava flow fronts and the summit vent during the effusive phase, back to fumaroles on the summit and cooling lava flows after the eruption ceased. The highest maximum FLIR-derived temperatures were recorded during the precursory (fumaroles) and effusive (lava) phases. Such results indicate that caution should be taken when using an average maximum temperature in models of effusion rates. Although these models can be highly accurate, they could be extracting temperatures from active lava flows, hot fumaroles, or simply exposed cracks. With lower-resolution satellite, discrimination of these features commonly becomes difficult.

To reduce the scatter and better assess overall temperature trends, the average surface temperatures of warm summit areas and, later, lava surfaces were measured (FLIR:T_{avg}, fig. 17; table 1). To further reduce meteorologic influences on FLIR-derived temperatures, the ambient background temperature near the summit (FLIR:T_{bg}, fig. 17; table 1) was subtracted from the average surface temperature (FLIR:T_{avg}). The resulting plot (FLIR:$T_{avg} - T_{bg}$, fig. 17) shows an increase in surface temperature during the precursory phase through the end of the effusive phase, with one anomalously low temperature likely due to poor observation conditions at the summit (February 8, 2006). The average surface temperature drops rapidly in late March, after the likely end of the effusive phase. Because the much larger ASTER pixels tend to integrate much of the variation in temperature documented by FLIR, maximum ASTER TIR (TIR:T_{max}, fig. 17; table 2) and ASTER SWIR (SWIR:T_{max}, fig. 17; table 2) -derived temperatures more closely follow the trend of FLIR:T_{avg} showing much elevated temperatures during the explosive through effusive phases. Deriving the average surface temperature from ASTER TIR (TIR:T_{avg}, table 2), the background-corrected plot (TIR:T_{avg}–T_{bg}, fig. 17) shows a steep rise in average surface temperature during the explosive and continuous phases, a slight decrease during the eruptive pause, an increase to the highest surface temperature during the effusive phase, and a steep drop in temperature after the eruption. The periods of rapid increase in ASTER-derived temperature appear to correlate with the higher effusion rates suggested by the cumulative erupted volumes estimated by Coombs and others (this volume).

Because Augustine Volcano is relatively close to communities in south-central Alaska, AVO was able to conduct many FLIR flights during the course of the eruption. However, most Alaskan eruptions occur in much more logistically difficult locations, making FLIR observations a rare occurrence outside the Cook Inlet region. high-resolution satellite TIR data from ASTER, in contrast, can be used to monitor any eruption no matter how remote. ASTER is well suited to volcanic observations because of its 15- to 90-m spatial resolution, its ability to be scheduled and point off-nadir, and its ability to collect multispectral data during both the day and the night. Aided by the high latitude of Augustine Volcano, ASTER was able to provide frequent repeat imaging as short as 1 day between scenes, with an average 6-day repeat during the height of eruptive activity in 2006 (fig. 17). A higher temporal resolution at ASTER TIR spatial resolution would be useful to more adequately establish volcano temperature trends, but owing to frequent clouds, volcanic emissions, and infrequent ASTER scheduling, better temporal coverage with high spatial resolution is not currently possible in Alaska for this type of detailed study.

Finally, ASTER also provides a means for reviewing volcano temperature trends since 2000. TES-derived kinetic temperature data extracted from 11 clear nighttime pre-eruption ASTER TIR images provide a timeline for low-temperature thermal activity at Augustine Volcano's summit (fig. 18). For the 6-year-period preceding the 2006 eruption, the background-adjusted ASTER TIR:T_{max} value averaged 5.4°C, with a standard deviation of 1.8°C. Over the same period, the background-adjusted ASTER TIR:T_{avg} averaged 1.9°C, with a standard deviation of 0.9°C. The sole pre-eruption ASTER TIR observation from December 20, 2005, 22 days before the first major explosions, had an ASTER TIR:T_{avg} value of 3.5°C at the summit, only about 1.6°C above the 6-year average but greater than 1σ.

Although ASTER did acquire another 3 daytime and 10 nighttime images during the year preceding the December 20 view, the volcano summit was obscured by clouds in all of them. The absence of cloud-free pre-eruption ASTER data demonstrates why future high-resolution satellite missions need to be designed to provide more frequent and regularly scheduled TIR acquisitions both day and night. The pre-eruption ASTER data, in combination with FLIR observations, suggest that if clear nighttime, high-resolution TIR data had been available days to weeks earlier, the anomalous summit temperatures might have been detected sooner than December 20, as occurred during both the 2005 and 2007 eruptions of Kliuchevskoi Volcano in Kamchatka, Russia (Ramsey and others, 2007; Rose and Ramsey, 2009).

Acknowledgments

We thank Matt Patrick and John Power for their timely reviews and suggestions. This research was supported by the USGS-AVO and NASA (grants NNG04GO69G and NNX-08AJ91G). ASTER data were obtained courtesy of NASA/GSFC/METI/ERSDAC/JAROS and U.S./Japan ASTER Science Team. We thank helicopter pilots Ken Deyoe and Rick Farish for safely and skillfully flying us to the volcano.

References Cited

Bailey, J.E., Dean, K.G., Dehn, J., and Webley, P.W., 2010, Integrated satellite observations of the 2006 eruption of Augustine Volcano, *in* Power, J.A., Coombs, M.L., and Freymueller, J.T., eds., The 2006 eruption of Augustine Volcano, Alaska: U.S. Geological Survey Professional Paper 1769 (this volume).

Ball, M., and Pinkerton, H., 2006, Factors affecting the accuracy of thermal imaging cameras in volcanology: Journal of Geophysical Research, v. 111, no. B11, p. 1–14.

Calvari, S., Spampinato, L., Lodato, L., Harris, A.J.L., Patrick, M.R., Dehn, J., Burton, M.R., and Andronico, D., 2005, Chronology and complex volcanic processes during the 2002–2003 flank eruption at Stromboli volcano (Italy) reconstructed from direct observations and surveys with a handheld thermal camera: Journal of Geophysical Research, v. 110, no. B2, p. 1–23.

Cervelli, P.F., Fournier, T., Freymueller, J.T., and Power, J.A., 2006, Ground deformation associated with the precursory unrest and early phases of the January 2006 eruption of Augustine Volcano, Alaska: Geophysical Research Letters, v. 33, L18304, doi: 10.1029/2006GL027219, 5 p.

Coombs, M.L., Bull, K.F., Vallance, J.W., Schneider, D.J., Thoms, E.E., Wessels, R.L., and McGimsey, R.G., 2010, Timing, distribution, and volume of proximal products of the 2006 eruption of Augustine Volcano, *in* Power, J.A., Coombs, M.L., and Freymueller, J.T., eds., The 2006 eruption of Augustine Volcano, Alaska: U.S. Geological Survey Professional Paper 1769 (this volume).

Dehn, J., Dean, K.G., Engle, K., and Izbekov, P., 2002, Thermal precursors in satellite images of the 1999 eruption of Shishaldin Volcano: Bulletin of Volcanology, v. 64, no. 8, p. 525–534.

Flynn, L.P., Harris, A.J.L., and Wright, R., 2001, Improved identification of volcanic features using Landsat 7 ETM+: Remote Sensing of Environment, v. 78, no. 1–2, p. 180–193.

Gillespie, A. R., Rokugawa, S., Matsunaga, T., Cothern, J. S., Hook, S. J., and Kahle, A. B. 1998, A temperature and emissivity separation algorithm for Advanced Spaceborne Thermal Emission and Reflection Radiometer (ASTER) images: Institute of Electrical and Electronics Engineers Transactions Geoscience Remote Sensing, v. 36, p. 1113–1126.

Harris, A.J.L., Dehn, J., and Calvari, S., 2007, Lava effusion rate definition and measurement; a review: Bulletin of Volcanology, v. 70, n. 1, p. 1–22.

Harris, A.J.L., Dehn, J., Patrick, M., Calvari, S., Ripepe, M., and Lodato, L., 2005, Lava effusion rates from hand-held thermal infrared imagery; an example from the June 2003 effusive activity at Stromboli: Bulletin of Volcanology, v. 68, p. 107–117.

Jacobs, K.M., and McNutt, S.R., 2010, Using seismic *b*-values to interpret seismicity rates and physical processes during the preeruptive earthquake swarm at Augustine Volcano 2005–2006, *in* Power, J.A., Coombs, M.L., and Freymueller, J.T., eds., The 2006 eruption of Augustine Volcano, Alaska: U.S. Geological Survey Professional Paper 1769 (this volume).

McGee, K.A., Doukas, M.P., McGimsey, R.G., Neal, C.A., and Wessels, R.L., 2010, Emission of SO_2, CO_2, and H_2S from Augustine Volcano, 2002–2008, *in* Power, J.A., Coombs, M.L., and Freymueller, J.T., eds., The 2006 eruption of Augustine Volcano, Alaska: U.S. Geological Survey Professional Paper 1769 (this volume).

Power, J.A., Nye, C., Coombs, M.L., Wessels, R.L., Cervelli, P.F., Dehn, J., Wallace, K.L., Freymueller, J.T., and Doukas, M., 2006, The reawakening of Augustine Volcano, Alaska: Eos, (American Geophysical Union Transactions), v. 87, p. 373–377.

Power, J.A., and Lalla, D.J., 2010, Seismic observations of Augustine Volcano, 1970–2007, *in* Power, J.A., Coombs, M.L., and Freymueller, J.T., eds., The 2006 eruption of Augustine Volcano, Alaska: U.S. Geological Survey Professional Paper 1769 (this volume).

Ramsey, M., and Dehn, J., 2004, Spaceborne observations of the 2000 Bezymianny, Kamchatka eruption; the integration of high-resolution ASTER data into near real-time monitoring using AVHRR: Journal of Volcanology and Geothermal Research, v. 135, no. 1–2, p. 127–146.

Ramsey, M.S., Dehn, J., Wessels, R.L., Byrnes, J., Duda, K., Maldonado, L., and Dwyer, J., 2004, The ASTER emergency scheduling system—A new project linking near-real-time satellite monitoring of disasters to the acquisition of high-resolution remote sensing data [abs.]: Eos (American Geophysical Union Transaction), v. 85, n. 47, Fall Meeting Supplement, Abstract SF23A-0026.

Ramsey, M.S., Duda, K., Dehn, J., Wessels, R., Skoog, R., and Rose, S., 2007, Application of the ASTER rapid response protocol for eruption detection and volcano monitoring: ASTER Science Workshop, p. 3–4.

Rose, S.R., and Ramsey, M.S., 2009, The 2005 eruption of Kliuchevskoi volcano; Chronology and processes derived from ASTER spaceborne and field-based data: Journal of Volcanology and Geothermal Research, v. 184, p. 367–380.

Schneider, D, Vallance, J., Wessels, R., Logan, M., and Ramsey, M., 2008, Use of thermal infrared imaging for monitoring renewed dome growth at Mount St. Helens, 2004, *in* Sherrod, D.R., Scott, W.E., and Stauffer, P.H. eds., A volcano rekindled; the renewed eruption of Mount St. Helens, 2004–2006: U.S. Geological Survey Professional Paper 1750, p. 347–359.

Thome, K., Palluconi, F., Takashima, T., and Masuda, K., 1998, Atmospheric correction of ASTER: IEEE Transactions on Geoscience and Remote Sensing, v. 36, no. 4, p. 1199–1211.

Vaughan, R.G., Hook, S.J., Ramsey, M.S., Realmuto, V.J., and Schneider, D.J., 2005, Monitoring eruptive activity at Mount St. Helens with TIR image data: Geophysical Research Letters, v. 32, L19305, doi:10.1029/2005GL024112.

Vaughan, R.G., and Hook, S.J., 2006, Using satellite data to characterize the temporal thermal behavior of an active volcano; Mount St. Helens, WA: Geophysical Research Letters, v. 33, L20303, doi:10.1029/2006GL027957.

Wright, R., and Flynn, L., 2003, On the retrieval of lava-flow surface temperatures from infrared satellite data: Geology, v. 31, p. 893–896.

Wallace, K.L., Neal, C.A., and McGimsey, R.G., 2010, Timing, distribution, and character of tephra fall from the 2005–2006 eruption of Augustine Volcano, *in* Power, J.A., Coombs, M.L., and Freymueller, J.T., eds., The 2006 eruption of Augustine Volcano, Alaska: U.S. Geological Survey Professional Paper 1769 (this volume).

Yamaguchi, Y., Kahle, A.B., Tsu, H., Kawakami, T., and Pniel, M., 1998, Overview of Advanced Spaceborne Thermal Emission and Reflection Radiometer (ASTER): Institute of Electrical and Electronics Engineers Transactions Geoscience Remote Sensing, v. 36, no. 4, p. 1062–1071.